

Old Dominion University

ODU Digital Commons

---

Chemistry & Biochemistry Theses & Dissertations

Chemistry & Biochemistry


---

Summer 2012

## Multidentate Resorcinarene Surfactants for the Phase Transfer of Metal Nanoparticles and Nanodiamonds: Applications in Catalysis and Diamond Film Growth

Vara Prasad Sheela  
*Old Dominion University*

Follow this and additional works at: [https://digitalcommons.odu.edu/chemistry\\_etds](https://digitalcommons.odu.edu/chemistry_etds)

 Part of the [Chemistry Commons](#), [Materials Science and Engineering Commons](#), and the [Nanoscience and Nanotechnology Commons](#)

---

### Recommended Citation

Sheela, Vara P. "Multidentate Resorcinarene Surfactants for the Phase Transfer of Metal Nanoparticles and Nanodiamonds: Applications in Catalysis and Diamond Film Growth" (2012). Master of Science (MS), Thesis, Chemistry & Biochemistry, Old Dominion University, DOI: 10.25777/g5v0-d993  
[https://digitalcommons.odu.edu/chemistry\\_etds/203](https://digitalcommons.odu.edu/chemistry_etds/203)

This Thesis is brought to you for free and open access by the Chemistry & Biochemistry at ODU Digital Commons. It has been accepted for inclusion in Chemistry & Biochemistry Theses & Dissertations by an authorized administrator of ODU Digital Commons. For more information, please contact [digitalcommons@odu.edu](mailto:digitalcommons@odu.edu).

**MULTIDENTATE RESORCINARENE SURFACTANTS FOR THE PHASE  
TRANSFER OF METAL NANOPARTICLES AND NANODIAMONDS:  
APPLICATIONS IN CATALYSIS AND DIAMOND FILM GROWTH**

by

Vara Prasad Sheela  
M.Sc. May 2007, Osmania University, India


A Thesis Submitted to the Faculty of  
Old Dominion University in Partial Fulfillment of the  
Requirements for the Degree of

MASTER OF SCIENCE

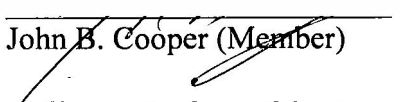
CHEMISTRY

OLD DOMINION UNIVERSITY  
August 2012

Approved by:

  
lasubramanian Ramjee (Director)

  
Kenneth G. Brown (Member)

  
John B. Cooper (Member)

  
Jennifer Poutsma (Member)

## **ABSTRACT**

### **MULTIDENTATE RESORCINARENE SURFACTANTS FOR THE PHASE TRANSFER OF METAL NANOPARTICLES AND NANODIAMONDS: APPLICATIONS IN CATALYSIS AND DIAMOND FILM GROWTH**

Vara Prasad Sheela  
Old Dominion University, 2012  
Director: Dr. Balasubramanian Ramjee

One main objective of the present work is to functionalize cuboctahedral platinum nanoparticles with various multidentate resorcinarene surfactants and study their influence in determining their catalytic activity. We hypothesized that catalytically active and recyclable catalysts can be achieved by incomplete yet strong passivation of the nanoparticle surfaces by using multidentate resorcinarene surfactants. We have developed phase transfer protocols for functionalizing cuboctahedral platinum nanoparticles with resorcinarene thiol or amine. Fluorescence assay confirmed that both these nanoparticles contained almost comparable unpassivated metal area. The activity of such phase transferred nanoparticles was tested in the catalytic hydrogenation of allyl alcohol. The conversion of allyl alcohol to propanol depended on both the nature and concentration of the stabilizing resorcinarene surfactant. While nanoparticles passivated with resorcinarene amine led to almost quantitative conversion under certain conditions, up to 58% conversion could be obtained even with resorcinarene thiol stabilized Pt nanoparticles. In the presence of excess surfactants, no changes in the size and shape of the nanoparticles were observed after catalysis. On the other hand, TEM analysis after catalysis showed that in the absence of excess surfactant, resorcinarene thiol stabilized nanoparticles were stable, while resorcinarene amine stabilized nanoparticles were

substantially aggregated. Overall, these results indicate that resorcinarene thiol can substantially increase the stability and hence the reusability of the nanoparticles without compromising on their catalytic activity.

Nanodiamonds have attracted lot of attention in recent years. However, their dispersion stabilization, or lack thereof, poses major limitations on their applications. Though covalent functionalization approaches have been developed to disperse nanodiamonds in non-polar organic solvents, there are certain inherent disadvantages. This work shows that resorcinarene amine surfactant can extract nanodiamonds of different sizes and shapes from aqueous to organic layer. Control experiments showed that both resorcinarene skeleton and amine groups are necessary for the extraction. Based on infrared spectroscopic analysis, we believe that these nanodiamonds are electrostatically stabilized by the resorcinarene amine surfactant. We in collaboration with Dr. Albin's group have showed that such resorcinarene surfactant stabilized nanodiamond dispersions can act as superior nucleation seeds for diamond film growth by chemical vapor deposition method.

This thesis is dedicated to my sister, Keshavi Sheela in her remembrance; I also dedicate this thesis to my parents and family members for being with me in all my endeavors.

## **ACKNOWLEDGMENTS**

I would like to express the deepest appreciation to my advisor Dr. Balasubramanian Ramjee. Without his guidance and persistent help this thesis would have not been possible. It is my great pleasure to thank my committee members for their contributions and suggestions in getting the thesis to a full form. I also thank Dr. Craig A. Bayse, Graduate Program Director for fuelling me up, to continue with my thesis. I would also like to thank my friend Ms. Swetha Polisetty for helping me in getting this thesis done.

## TABLE OF CONTENTS

	Page
LIST OF FIGURES .....	viii
 Chapter	
I. INTRODUCTION .....	1
SYNTHESIS OF NANOPARTICLES .....	3
PHASE TRANSFER OF NANOPARTICLES .....	4
ROLE OF LIGANDS IN CATALYSIS .....	6
SHAPE AND SIZE EFFECTS OF NANOPARTICLES IN CATALYSIS .....	7
INTRODUCTION TO NANODIAMONDS AND THEIR APPLICATIONS .....	9
DISPERSION STABILIZATION AND FUNCTIONALIZATION OF NANODIAMONDS .....	10
II. MULTIDENTATE RESORCINARENE SURFACTANTS FOR THE PHASE TRANSFER OF METAL NANOPARTICLES AND NANODIAMONDS: APPLICATIONS IN CATALYSIS AND DAIMOND FILM GROWTH.....	14
INTRODUCTION TO RESORCINARENE .....	14
MULTIDENTATE RESORCINARENE SURFACTANTS FOR METAL NANOPARTICLE STABILIZATION.....	15
INFLUENCE OF RESORCINARENE SURFACTANT LIGANDS ON THE CATALYTIC ACTIVITY OF SHAPE SELECTED PLATINUM NANOPARTICLES.....	17
SYNTHESIS OF RESORCINARENE SURFACTANTS .....	19
INITIAL WORK.....	21
SYNTHESIS AND PHASE TRANSFER OF CTAB STABILIZED CUBOCTAHEDRAL AND CUBIC PLATINUM NANOPARTICLES.....	22
SOLVENT EFFECT ON PHASE TRANSFER .....	26
PRECIPITATION-REDISPERSION OF RESORCINARENE SURFACTANT EXTRACTED NANOPARTICLES.....	28
AVAILABLE SURFACE AREA FOR CATALYSIS .....	29
CATALYTIC HYDROGENATION OF ALLYLALCOHOL TO PROPANOL USING RESORCINARENE SURFACTANT STABILIZED CUBOCTAHEDRAL NANOPARTICLES .....	30
STABILIZATION AND PHASE TRANSFER OF NANODIAMONDS .....	35
UNDERSTANDING THE EXTRACTION OF NANODIAMONDS BY RESORCINARENE AMINE SURFACTANT.....	38
EXTRACTION OF NANODIAMONDS FROM VARIOUS COMMERCIAL SOURCES .....	40

	Page
DIAMOND FILM GROWTH USING RESORCINARENE AMINE ENCAPSULATED NANODIAMONDS AS NUCLEATING AGENTS .....	43
EXPERIMENTAL SECTION .....	46
III. CONCLUSIONS.....	57
CONCLUSIONS FOR CATALYSIS WORK.....	57
CONCLUSIONS FOR NANODIAMOND WORK.....	58
REFERENCES .....	59
APPENDIX.....	63
VITA .....	64



## LIST OF FIGURES

Figure	Page
1. General structure of a resorcinarene <b>1</b> .....	14
2. General structure of a resorcinarene cavitand <b>2</b> .....	15
3. TEM image of PdPt bimetallic nanoparticles .....	17
4. Resorcinarene thiol <b>3</b> and resorcinarene amine <b>4</b> surfactants.....	18
5. Synthesis of resorcinarene thiol and amine surfactants .....	20
6. TEM image of PVP stabilized tetrahedral platinum nanoparticles.....	21
7. Low (a) and High (b) resolution TEM images of CTAB stabilized cuboctahedral platinum nanoparticles.....	23
8. Photographs of resorcinarene thiol (left) and resorcinarene amine (right) extracted cuboctahedral platinum nanoparticles.....	24
9. TEM images of (a) resorcinarene thiol, (b) resorcinarene amine extracted cuboctahedral platinum nanoparticles and (c) resorcinarene thiol extracted cubic platinum nanoparticles .....	25
10. <sup>1</sup> H-NMR spectra of resorcinarene thiol extraction of cuboctahedral platinum nanoparticles carried out in (a) toluene and (b) chloroform .....	27
11. Surface area measurement of platinum nanoparticles stabilized with resorcinarene thiol <b>3</b> and resorcinarene amine <b>4</b> .....	30
12. <sup>1</sup> H-NMR spectra of the hydrogenation reactions catalyzed by platinum nanoparticles stabilized with (a) resorcinarene thiol (unprecipitated sample) and (b) resorcinarene amine (precipitated sample).....	32
13. TEM analysis of cuboctahedral platinum nanoparticles after catalysis.....	34
14. Nitrogen containing model surfactants .....	37
15. Four-month-old dispersions of resorcinarene amine stabilized Microdiamant nanodiamonds in tetrahydrofuran (left) and toluene (right) .....	38
16. FTIR spectra of resorcinarene amine encapsulated and precipitated Microdiamant nanodiamond dispersions .....	40

	Page
17. Resorcinarene amine extracted (a) Microdiamant, (b) Altai and (c) Dynalene nanodiamonds .....	41
18. TEM analysis of resorcinarene amine extracted (a - b) Altai, (c - d) Dynalene, (e - f) Microdiamant and (g - h) DuPont nanodiamonds .....	42
19. SEM (a - c) and AFM (d - e) analysis of diamond films grown with resorcinarene amine encapsulated nanodiamonds (a and d) and unmodified Microdiamant nanodiamonds (b and e) as nucleation seeds and those grown without a nucleating agent (c) .....	45
20. <sup>1</sup> H-NMR of resorcinarene benzyl thiol <b>3</b> .....	51
21. <sup>13</sup> C-NMR of resorcinarene benzyl thiol <b>3</b> .....	52
22. FTIR of resorcinarene benzyl thiol <b>3</b> .....	53
23. <sup>1</sup> H-NMR of resorcinarene amine <b>4</b> .....	55
24. <sup>13</sup> C-NMR of resorcinarene amine <b>4</b> .....	55
25. FTIR of resorcinarene amine <b>4</b> .....	56

## CHAPTER I

### INTRODUCTION

Nanoparticles, by definition have at least one dimension under 100 nm. In the field of nanoscience, metal nanoparticles have gained interest due to their unique size and shape dependent optical,<sup>1,2</sup> catalytic<sup>3</sup> and electronic<sup>4</sup> properties which differ from bulk materials. These exclusive properties of metal nanoparticles are useful in catalysis,<sup>5,6</sup> electrocatalysis,<sup>7</sup> bioimaging and therapeutic applications.<sup>8</sup>

Typically, the ratio of surface area and volume is related inversely to the radii of the nanoparticle. Nanoparticles, with their relatively smaller dimensions, have a larger percentage of surface atoms with high surface energy<sup>9</sup> when compared to the total number of atoms. Further, the nanoparticles are attracted to each other due to van der Waals forces. Hence, in the absence of appropriate stabilization, nanoparticles have a greater tendency to aggregate resulting in the loss<sup>10</sup> of their exclusive properties.<sup>1,2,3</sup> The different strategies used to stabilize nanoparticles are:

**(1) Electrostatic stabilization.** In this approach the attractive van der Waals forces are counter balanced by the repulsive coulombic forces by adsorbed ions. Negatively charged ionic compounds are adsorbed on to the positively charged metal surfaces. Further adsorption of oppositely charged counter ions onto the adsorbed ions results in the formation of an electric double layer around the nanoparticles. This adsorption of ions provides the coulombic repulsive forces between the particles and prevents nanoparticle aggregation. When the electric potential between the double layer is high, particles are stabilized electrostatically. For example ionic compounds such as halides<sup>11,12</sup> and

carboxylates<sup>13</sup> (sodium citrate where  $\text{Na}^+$  is used as counter-cations) have been used to stabilize nanoparticles.

**(2) Steric stabilization.** In this approach, macromolecules are adsorbed on nanoparticles by partial ligation and provide a protective layer which prevents the nanoparticles from aggregation. In addition to free energy considerations arising out of macromolecular adsorption, nanoparticles are also stabilized by the osmotic repulsion effects (solvents will intervene and separate two aggregating nanoparticles). Polymers<sup>14,15</sup> and dendrimers<sup>6</sup> are good examples of the steric stabilization strategy. Compared to electrostatic stabilization, which is mainly used in aqueous phase, steric stabilization can be used both in aqueous and non-aqueous phases.

**(3) Electrosteric stabilization.** This approach combines the benefit of both electrostatic and steric stabilization. Ionic surfactants and polyoxoanions<sup>16</sup> stabilize the nanoparticles electrosterically. Ionic surfactants have head groups, which help in forming a double layer as in electrostatic stabilization. The side chain of the surfactant further provides steric repulsion and prevents the nanoparticles from aggregation.

**(4) Ligand stabilization.** Metal nanoparticles can be prevented from aggregation by coordination of nanoparticles with ligands. Various linear alkyl chain organic compounds can be used for this type of stabilization. Alkanethiols<sup>17</sup> and amines<sup>13,18</sup> are good examples. Ligand stabilization results in the formation of self-assembled monolayers (SAM's). Metal surfaces covered with a single layer of ligand molecules are self-assembled monolayers. Hence self-assembly results in the definitive structure for the nanoparticles.

## Synthesis of Nanoparticles

Nanoparticles can be synthesized by two general approaches.<sup>19</sup> The top-down approach or physical method is a process where the bulk metals are broken down to nano-sized particles. The top-down approach can be achieved by a variety of methods such as laser ablation, arc discharge and evaporation.<sup>20</sup> Monodisperse bismuth nanospheres<sup>21</sup> were synthesized by emulsifying the drops of molten bismuth powders and then quenching them in cold ethanol. This method was also employed for a range of metals such as Pb, Sn, In, Cd and their alloys. A limitation of this approach is that the size distribution of nanoparticles synthesized is very broad.<sup>19</sup>

The bottom-up approach or chemical method is the most commonly used approach for the synthesis of nanoparticles.<sup>22,12</sup> Brust-Schffrin biphasic synthesis of nanoparticles is one of the most important examples of this approach. Briefly, metal ions in the aqueous phase are transferred to the organic phase by tetraoctylammonium bromide (TOABr), a phase transfer agent. Then the metal ions in the organic phase are reduced under biphasic conditions by using aqueous sodium borohydride. This reaction is usually carried out in the presence of dodecanethiol, producing thiol stabilized metal nanoparticles.<sup>23</sup> Nanoparticles of various metals such as Au,<sup>23</sup> Pt,<sup>12</sup> Pd,<sup>24</sup> Ag<sup>25</sup> etc., have been synthesized by this approach. Another good example is the synthesis of citrate stabilized gold nanoparticles by the Turkevich<sup>26</sup> method. In this method, gold salt is reduced by sodium citrate solution in an aqueous media resulting in deep wine red colored citrate stabilized gold nanoparticles.

The synthesis of metal nanoparticles using the chemical method can be carried out either in aqueous or non-aqueous media. Each of these synthetic media have their own

merits and demerits.<sup>27</sup> Often, the medium where the nanoparticles are dispersed can pose certain fundamental limitations. For example, the catalytic nanoparticles synthesized in aqueous medium can't be used for the synthetic transformation of non-polar organic compounds due to solubility issues. Likewise, nanoparticles synthesized in organic media cannot be used for biological imaging. Hence, there is a need to develop methods to phase-transfer such nanoparticles into another medium for applications.

### **Phase Transfer of Nanoparticles**

In terms of nanoscience, phase transfer can be defined as transfer of nanoparticles from the aqueous to the organic phase or vice-versa without harming the properties of the nanoparticles. Phase transfer of nanoparticles can be achieved by methods such as ligand exchange and electrostatic interactions.

**Ligand Exchange Mediated Phase Transfer.** Ligand exchange is a process where the ligands stabilizing the nanoparticles are replaced with other ligands. The important aspect of ligand-exchange-mediated<sup>28</sup> phase transfer is that, the incoming ligand should bind equally or even stronger than the stabilizing ligand on the nanoparticle surface. In 1997, Rao and coworkers<sup>29</sup> developed a phase-transfer approach for the transfer of nanoparticles from aqueous to organic phase which used concentrated hydrochloric acid as a phase-transfer agent. By using this approach, they have prepared alkane thiol stabilized gold (Au), silver (Ag) and platinum (Pt) nanoparticles. By shaking the biphasic mixture (aqueous and chloroform) of the inclusion complex,<sup>30</sup> gold nanoparticles synthesized in the aqueous solution were transferred to the organic phase. In another study, Crooks *et. al.*<sup>31</sup> have shown that by using phase transfer, even dendrimer

encapsulated nanoparticles (DEN's) can be transferred from the aqueous layer to the organic layer by the use of alkane thiol ligands.

By shaking the mixture of gold aqueous sol with an organic solution of a particular amine, gold nanoparticles of various sizes were stabilized by alkyl amines<sup>32</sup> of various chain lengths and extracted to the organic phase. The authors have found that for smaller sizes of nanoparticles, even shorter chain length ligands can lead to complete transfer of nanoparticles from aqueous to organic phase.

**Phase Transfer by Electrostatic Interactions.** Electrostatic interactions between the phase transfer agents and stabilizers on the metal nanoparticles have been used to transfer nanoparticles from the aqueous to the organic phase or vice-versa. Cheng *et. al.*<sup>11</sup> have extracted gold nanoparticles of less than 5 nm by electrostatic interactions between tetraoctylammonium ions and citrate ions (on the surface of the nanoparticles). A similar approach was also used to phase-transfer Ag nanoparticles using negatively charged oleate ions.<sup>25</sup>

**Phase Transfer from Organic to Aqueous Phase.** Ligand exchange of hydrophobic gold nanoparticles with poly(ethylene glycol) grafted hyperbranched poly(amidoamine) copolymer<sup>33</sup> resulted in the phase-transfer of nanoparticles from the organic to the aqueous phase. In this case, the presence of poly(ethylene glycol) groups enabled the nanoparticles to solubilize in water. This reaction was done at 35 °C for 24 h. Another example is the formation of a donor-acceptor complex<sup>34</sup> between 4-dimethylaminopyridine (as donor) and a nanoparticle surface (as acceptor). Au and Ag nanoparticles were transferred from the organic to the aqueous phase in an hour at room temperature using donor acceptor complex formation.

Each of the procedures described above has its own limitations. Nanoparticle size dependent phase transfer is a major limitation.<sup>11,35</sup> It is worth noting that simple alkyl amines (even with a chain length of 18 carbons) cannot completely extract gold nanoparticles over 18 nm in dimensions.<sup>32</sup> Also, the use of conc. HCl<sup>29</sup> as phase transfer agent might be problematic when attempting to stabilize the nanoparticles with various ligands such as amine or phosphine. Another limitation of some of the phase-transfer methods includes prolonged duration time.<sup>30</sup> Using phase transfer method nanoparticles can be made either hydrophobic or hydrophilic for their widespread applications in catalysis,<sup>36</sup> biomedical,<sup>37</sup> and formation of nanoparticle films, which are further used in nanodevices<sup>38</sup> etc.

### **Role of Ligands in Catalysis**

The attractive feature of nanoparticle mediated catalysis is the ability to correlate catalytic activity, selectivity, and stability with the tunable physical parameters of size, shape, surface composition and support. Ligand stabilized nanoparticles are generally called monolayer protected clusters. The Brust-Schffrin<sup>23</sup> method is the most promising method to synthesize monolayer protected clusters. It is well documented in the literature that catalysis is a surface property.<sup>39,40,41,42</sup> Catalysis with ligand passivated metal nanoparticles offers a unique opportunity to study size and shape effects in catalysis by eliminating the influence of support. However, this poses a formidable challenge, as the stabilization of the nanoparticle core which prevents irreversible aggregation, must be effectively balanced with its reactivity towards substrates i.e., catalytic activity.



Often catalytic nanoparticles are passivated with weakly-binding surfactants like polymers or amine surfactants as strongly binding surfactants such as thiol typically results in either reduced catalytic activity or none at all.<sup>16</sup> The effect of stabilizers on catalytic activity was studied by Li and El-Sayed<sup>24</sup> for the Suzuki reaction with palladium nanoparticles as the catalyst. It was shown by the authors that the ligands that stabilize the nanoparticles the most also make them catalytically less active. In a similar vein, Korgel and coworkers have shown that the stabilization by a ligand head group and catalytic activity of ligand stabilized nanoparticles are inversely-related in the catalytic reduction of 1-decene to decane by iridium nanoparticles.<sup>43</sup> Though traditionally considered a catalyst poison, thiolate stabilized platinum monolayer protected clusters did show some (reduced) catalytic activity in hydrogenation reactions.<sup>44</sup> In addition to modulating the catalytic activity, the ligand largely determines the solubility properties of nanoparticles and may restrict their wider applicability, often requiring modifications. Note that the above investigations of ligand effects were carried out with nanoparticles of different sizes.<sup>43</sup>

### **Shape and Size Effects of Nanoparticles in Catalysis**

Nanoparticle shape<sup>14</sup> dependent catalysis is an emerging topic of fundamental importance. Nanostructures bound by high-index planes<sup>45</sup> contain a higher percentage of defect sites including steps, ledges and kinks, and exhibit enhanced catalytic activity. Unusual tetrahedral<sup>46</sup> shaped platinum nanocrystals with exposed high-index facets have shown enhanced catalytic activity (up to 400%) compared to equivalent platinum surface areas. Different facets of platinum nanoparticles have in fact catalyzed different

types of reactions, and even for the same reaction, there are facet dependent differences in the catalytic profiles.<sup>14,47</sup> These reactivity differences are usually attributed to the differences in nanoparticle binding sites. Narayanan and El-Sayed have compared shape effects of tetrahedral and cubic platinum nanoparticles on the catalytic activity of the electron transfer reaction between hexacyanoferrate (III) and thiosulfate ions. Tetrahedral nanoparticles having sharp corners and edges are catalytically more active when compared to the cubic nanoparticles.

Benzene hydrogenation, a structure sensitive reaction using shape-selective cubic and cuboctahedral platinum nanoparticles was studied by Bratlie *et. al.*<sup>48</sup> Reactions in which the turn over frequency<sup>49</sup> is greater on certain surface sites than others are referred to as structure sensitive reactions. Both cyclohexane and cyclohexene were formed when cuboctahedral platinum nanoparticles consisting of Pt(100) and Pt(111) facets were used. Only cyclohexane was formed when cubic Pt NPs consisting solely of Pt(100) facets were used. Similar studies done on palladium<sup>50</sup> and rhodium<sup>51</sup> nanoparticles also showed the shape dependent nature of catalysis. Note that a systematic study of ligand effects on the shape of metal nanoparticles in catalysis has not been reported. This could be due to the fact that *a priori* synthesis of shape selected nanoparticles with tailor-made surfactants may not be a straight forward task, without affecting shape. Hence, there is a need to systematically study the ligand effects on the catalytic activity of shape-selected nanoparticles.

## Introduction to Nanodiamonds and their Applications

Nanodiamonds are another important class of nanomaterials and have attracted a lot of attention in recent years. They have bulk diamond like structure and properties and have typical dimensions of under 100 nm. The word diamond is obtained from Greek *adamas*,<sup>52</sup> which means indestructible. Nanodiamonds<sup>53</sup> are known for their properties such as high biocompatibility and low cytotoxicity,<sup>54,55</sup> wide band gap, chemical inertness, hardness,<sup>52</sup> thermal conductivity, electrical and optical properties.<sup>53,56</sup>

Artificial nanodiamond synthesis was not done until the middle of 20<sup>th</sup> century. There exist diverse<sup>57,58</sup> methods for the synthesis of nanodiamonds such as gas-phase nucleation, chlorination of carbides, and high pressure high temperature graphite transformation within a shock wave or carbon condensation during explosive detonation. Based on the size, nanodiamonds are classified in to 3 types.

- (i) Nanocrystalline diamond particles:<sup>53</sup> These are several nanometers (10 - 100 nm) in size and can be either monocrystalline or polycrystalline in nature. Processing of micron-sized monocrystalline (byproduct of natural diamond or HPHT synthesis) and polycrystalline diamond (by shock synthesis)<sup>59</sup> produces nanocrystalline diamond particles.
- (ii) Ultrananocrystalline diamond particles: These have a typical dimension of ~ 10 nm, and are synthesized by the popular detonation approach. As the size of the primary particles depends on weight of explosive charge there is no specific maximum size for these nanodiamonds and they are vendor specific with an average size of 3.5 to 6 nm.
- (iii) Diamondoids:<sup>60</sup> These are much smaller in size (1 - 2 nm) and their surface is terminated with hydrogen. These diamondoids are of two types (a) higher diamondoids

extracted from petroleum and (b) lower diamondoids extracted from crude oil. Based on the extraction of diamondoids from various sources, lower diamondoids exist more compared to the higher diamondoids.

Nanodiamonds have found wide spread applications from drug delivery platforms,<sup>61,62</sup> composite materials,<sup>63</sup> electronic devices to magnetic and quantum applications.<sup>64,65</sup> For example, Zhang *et. al.*<sup>66</sup> have reported that nanodiamonds (NDs) can be used as gene delivery vehicles. Using HeLa cells, the authors have shown that ND-PEI800 (nanodiamond polyethyleneimine complex) shows 70-fold higher gene transfection efficiency compared to PEI800 alone. A Pd catalyst<sup>67</sup> prepared using detonation nanodiamond (DND) as a support showed that nanodiamonds can act as support for the metals in hydrogenation reactions. Compared to C<sub>60</sub> fullerenes and carbon nanotubes (CNT's), nanodiamond support shows high reactivity for hydrogenation.

### **Dispersion Stabilization and Functionalization of Nanodiamonds**

During the synthesis of nanodiamonds by various methods (especially by the detonation method) sp<sup>2</sup> hybridized carbon is also produced along with sp<sup>3</sup> hybridized carbon in nanodiamond particles. The air oxidation method was employed by Osswald *et. al.*<sup>68</sup> for selectively removing the sp<sup>2</sup> hybridized amorphous carbon material. Note that the presence of small amounts of graphitic material on nanodiamond surfaces results in the agglomeration of nanodiamonds.<sup>69</sup> Although agglomerated nanodiamonds are used for selective separation of phenolic compounds<sup>70</sup> and in chemotherapeutic drug delivery,<sup>61</sup> the de-agglomeration of nanodiamonds is required for various applications.

Mechanical methods, such as wet<sup>71,72</sup> and dry<sup>73</sup> milling have been developed for de-agglomeration of nanodiamonds. Kruger *et. al.*<sup>71</sup> showed that by using a stirred media milling method, core aggregates with a diameter range of 100 - 200 nm can be disintegrated to primary particles of 4 - 5 nm in diameter. One of the major problems associated with this method is the contamination of silica in the milled diamond samples.

The other disadvantage of this method is that it results in larger (2.3  $\mu\text{m}$ ) nanodiamond aggregates. Similar to the silica approach, an improved method called bead assisted sonic disintegration (BASD) was developed by Osawa *et. al.*<sup>72</sup> Using the BASD method, primary diamond particles can be dispersed in highly polar alcohols and dimethyl sulfoxide (DMSO). Although the BASD method has become popular for disintegration of detonation nanodiamonds, there are side effects<sup>74</sup> such as contamination by zirconia and generation of graphitic layers.

In contrast to wet milling methods<sup>71,72</sup> a contaminant free and cost effective dry milling method was developed by Gogotsi.<sup>73</sup> Nanodiamond aggregates (with dimensions of 1000 nm) were broken down to primary particles using micrometer sized sucrose or sodium chloride. Further, adjusting the pH of aqueous diamond suspensions of milled powder to 11.4, results in a decrease in the size of the larger aggregates (100 - 200 nm) to <10 nm.

Using mechanical treatments it is possible to break the aggregates, but the disadvantage is that they have a tendency to reaggregate upon redispersion.<sup>71</sup> A mechanochemical treatment was implemented by Xu and coworkers<sup>75</sup> to prepare a stable nanodiamond dispersion, where the mechanical treatment disintegrates the aggregates,

and surfactant (sodium oleate) is adsorbed on to the nanodiamond surface and stabilizes the nanodiamonds. A major limitation of this method is that it is pH dependent.

Apart from the mechanical methods, Xu and Xue<sup>76</sup> used a graphitization-oxidation method for de-aggregation of detonation nanodiamonds. Using this method, a nanodiamond aggregate of ~ 1000 nm was disintegrated to diameters less than 50 nm. However, note that this method uses elevated temperatures of 1000 °C for graphitization and 450 °C for oxidation.

Other than mechanical and mechano-chemical techniques both covalent and non-covalent functionalization approaches have been used to disperse and stabilize the nanodiamonds in aqueous and organic media. Depending on the purification<sup>77,78</sup> techniques employed during the nanodiamond synthesis, there exist various functional groups on the surface of nanodiamond. Commercially available detonation nanodiamonds are oxidized resulting in various functional groups<sup>79</sup> such as carboxylic acids, carbonyls and alcohols. Presence of these functional groups makes the surface of the nanodiamond hydrophilic in nature which enables hydrogen bonding with polar compounds. In addition, the presence of functional groups allows biomolecules to be immobilized on the nanodiamond surface both covalently<sup>80</sup> and non-covalently.<sup>81</sup>

Various functionalization approaches have also been developed to aid the dispersion stabilization of nanodiamonds. Liu *et. al.*<sup>82</sup> modified the surface of nanodiamond powders by covalent functionalization with fluorine and hydrogen gases at high temperatures (150 - 470 °C). The fluorinated nanodiamonds thus synthesized were further functionalized with nucleophilic reagents to synthesize alkyl, amine or acid

terminated nanodiamonds. These functionalized nanodiamonds were soluble in various solvents such as ethanol, 2-propanol and tetrahydrofuran.

In addition, blue fluorescent nanodiamonds (ND-ODA) were synthesized by Mochalin *et. al.*<sup>83</sup> by covalently linking octadecylamine (ODA) to nanodiamond (ND) particles through an amide bond. The presence of hydrocarbon chains enables the solubilization of ND-ODA in various organic solvents such as chloroform, dichloromethane, toluene, benzene etc. Surface functionalization of nanodiamonds with both polar and non-polar functionalities was developed by Chang and coworkers.<sup>84</sup> The authors have surface graphitized commercially available nanodiamonds, which were further surface grafted with monomers of various functionalities in tetrahydrofuran or aqueous solutions.

A non-covalent strategy<sup>85</sup> was developed for dispersing the nanodiamonds in organic solvents. Oleylamine was used as the dispersant, where an amino group serves as an electron donor for Lewis acid sites of carboxylic acid groups on the oxidized nanodiamonds. A major limitation of this approach is that the dispersed nanodiamonds were stable only for a week. In summary, the major disadvantages<sup>84</sup> of the current functionalization approaches are that they:

- (i) involve use of toxic gases<sup>82</sup> and strong acids
- (ii) involve multiple steps<sup>83</sup>
- (iii) use elevated temperatures<sup>84</sup> and
- (iv) are time consuming processes<sup>86</sup>

Hence, there is a need to develop an alternate, rapid, and simple method to disperse and stabilize nanodiamonds.

## CHAPTER II

### MULTIDENTATE RESORCINARENE SURFACTANTS FOR THE PHASE TRANSFER OF METAL NANOPARTICLES AND NANODIAMONDS: APPLICATIONS IN CATALYSIS AND DIAMOND FILM GROWTH

#### Introduction to Resorcinarene

Resorcinarenes **1** (Figure 1) are macrocyclic molecules, often used in supramolecular chemistry. They can be synthesized in a single step by an acid-catalyzed condensation between an aldehyde (aliphatic or aromatic) and resorcinol in the presence of alcohol/HCl under reflux conditions.

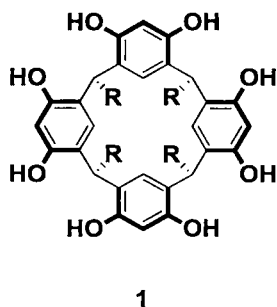


**Figure 1.** General structure of a resorcinarene **1**.

Resorcinarene cavitands **2** ( $R^1 = \text{Br}$  or  $\text{H}$  or alkyl) (Figure 2) were formed by linking the adjacent phenolic groups of resorcinarene **1**. The term cavitand was coined by Cram<sup>87</sup> for organic compounds having a concave cavity to accommodate other molecules or ions.



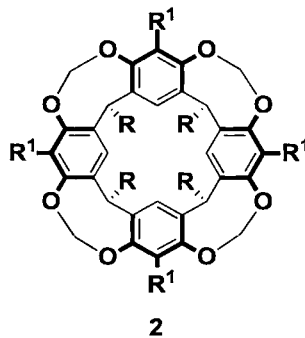


**Figure 2.** General structure of a resorcinarene cavitand 2.

The ease of functionalization at the upper and lower rims of the resorcinarenes have made them useful in the formation of capsules,<sup>88</sup> nanoparticles,<sup>89</sup> multiwalled microtubes<sup>90</sup> etc. Balasubramanian *et. al.* have shown that by employing resorcinarene tetraalkene tetrathiol (Figure 2) (2.  $R^1 = SH$ ), resorcinarene nanocapsules can be formed using thiol-ene photopolymerization in the absence of templates.<sup>91</sup>

### Multidentate Resorcinarene Surfactants for Metal Nanoparticle Stabilization

Wei and coworkers have shown that resorcinarenes, with their large head groups and flexible hydrocarbon tails, can act as efficient steric stabilizers of gold nanoparticles.<sup>92</sup> They suggested that the multiple (Au-O) interactions between the surface of the gold nanoparticles and the hydroxyl groups present on the head group of the resorcinarene surfactant caused the stabilization. Surface-enhanced raman spectroscopic analysis provided further evidence for the chemisorption of resorcinarene surfactant on to the gold nanoclusters. These nanoparticle dispersions had limited stability and the resorcinarene surfactant could be readily displaced by linear thiols.

Balasubramanian *et. al.*<sup>93</sup> reported the use of thiolated resorcinarenes and their utility in the phase-transfer of gold nanoparticles from the aqueous to the organic phases. They mixed aqueous citrate stabilized gold colloid dispersions with an equal volume of resorcinarene thiol surfactant in THF. To this one phase mixture, addition of a water-insoluble co-solvent resulted in the phase-transfer of nanoparticles into the organic phase. They noted that solvent played a major role in the above extraction procedure. For example, when compared to non-polar hexanes as co-solvent, toluene could extract larger sized colloids into the organic phase, and the use of chloroform could further extend the utility of this approach. Using this approach they could extract gold colloids of dimensions up to 87 nm. Occasionally, a minimum amount of TOABr (typically < 3 mol% when compared to resorcinarene thiol) was needed for the complete extraction of the gold nanoparticles into the organic phase. These resorcinarene thiol passivated nanoparticle dispersions in non-polar organic solvents were more stable than the parent resorcinarene stabilized dispersions and could be precipitated-redispersed without irreversible aggregation.

This phase transfer was explained on the basis of the chemisorptive properties of the resorcinarene surfactant head groups. Their work showed that nature of the head group (i.e., CH<sub>2</sub>SH or SH) attached to the resorcinarene skeleton played a critical role in determining the dispersion stability of the passivated nanoparticles. The presence of the CH<sub>2</sub> spacer in the former resulted in more robust dispersions when compared to the latter (SH) functional group. Using x-ray photoelectron spectroscopic studies, they showed that almost 2/4 thiol groups present on the surfactants can bind strongly to gold surfaces in the case of the resorcinarene surfactant functionalized with CH<sub>2</sub>SH groups.

Recent work from our research group showed that a somewhat related resorcinarene amine **4** surfactant can influence the shape and composition of PdPt bimetallic nanoparticles.<sup>94</sup> TEM analysis (Figure 3) had shown that the nanoparticles are dominantly V-shaped or variants on the V-shape. From mechanistic investigations it was concluded that resorcinarene amine plays a vital role in the formation of the V-shaped nanoparticles.

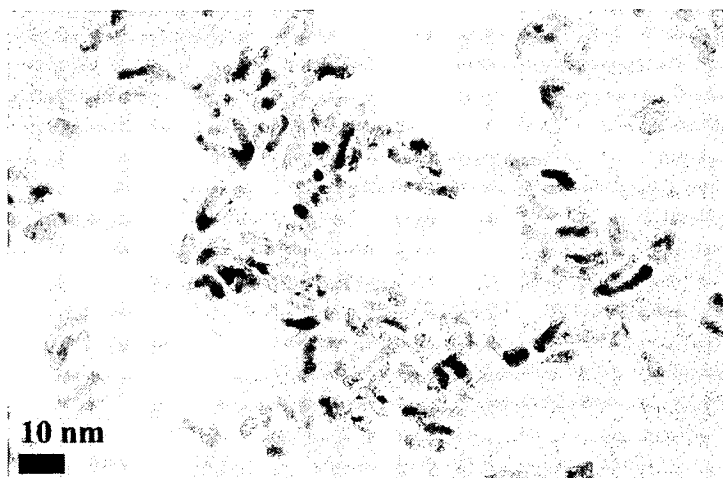


**Figure 3.** TEM image of PdPt bimetallic nanoparticles.

### **Influence of Resorcinarene Surfactant Ligands on the Catalytic Activity of Shape Selected Platinum Nanoparticles**

We envisaged that the formidable challenge of balancing the nanoparticle core stabilization with its catalytic activity, towards generating catalytically active and recyclable catalysts can be achieved by incomplete yet efficient strong passivation of nanoparticle surfaces by using multidentate resorcinarene surfactants. Despite the

advantages of using resorcinarenes for metal nanoparticle stabilization,<sup>92,93,95</sup> most of the work has focused on Au nanoparticles.

We propose to systematically study the ligand effects of resorcinarene based surfactants (Figure 4) in determining the catalytic activity of shape selected Pt nanoparticles. We hypothesized that both resorcinarene thiol **3** and amine **4** surfactants should offer a comparable amount of unpassivated metal surfaces for potential catalysis. In the past, Kaifer and coworkers<sup>96</sup> have shown that thiolated cyclodextrin, a multidentate surfactant, can be effectively used for stabilizing Pt and Pd nanoparticles without loss of catalytic activity. Note that such a study primarily dealt with spherical nanoparticles and did not specify about the stability of the nanoparticles during and after catalysis. Also, a detailed ligand effect study was lacking. To unambiguously probe the ligand effects, without any variations in the size or the shape of nanoparticles, we chose to use phase-transfer as a strategy for these studies.

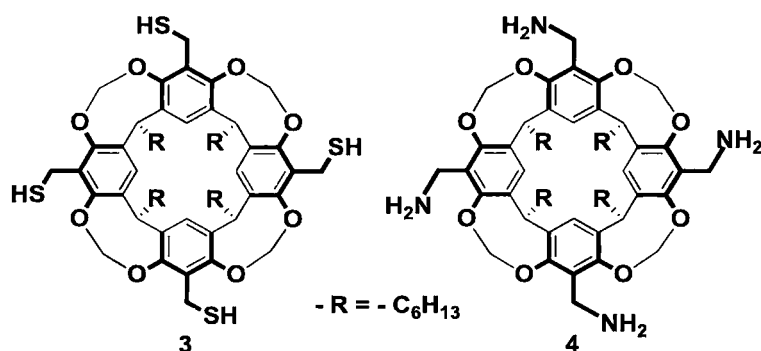


**Figure 4.** Resorcinarene thiol **3** and resorcinarene amine **4** surfactants.

### Synthesis of Resorcinarene Surfactants

Resorcinarene thiol **3** was synthesized by following the procedure of Balasubramanian *et. al.*<sup>93</sup> Briefly, this synthesis was done in a four step process. Resorcinarene **5** was synthesized from 2-methyl resorcinol and heptanal, under acidic conditions, followed by the covalent linking of neighboring phenolic hydroxyl groups with bromochloromethane in the presence of cesium carbonate to yield resorcinarene cavitand **6**. This cavitand **6** was then subjected to bromination with N-bromosuccinimide to yield bromomethylcavitand **7**. Bromomethylcavitand was treated with thiourea to generate resorcinarene thiol **3** (Figure 5).

Resorcinarene amine **4** was synthesized<sup>97</sup> by slightly modifying the literature procedure.<sup>98</sup> Reaction of **7** with potassium phthalimide and cetyltrimethylammonium bromide (CTAB), the phase-transfer catalyst, in refluxing toluene gave resorcinarene phthalimido methyl cavitand **8**. These phthalimido groups were removed by treatment with hydrazine hydrate in refluxing ethanol/THF to give resorcinarene amine **4** (Figure 5).

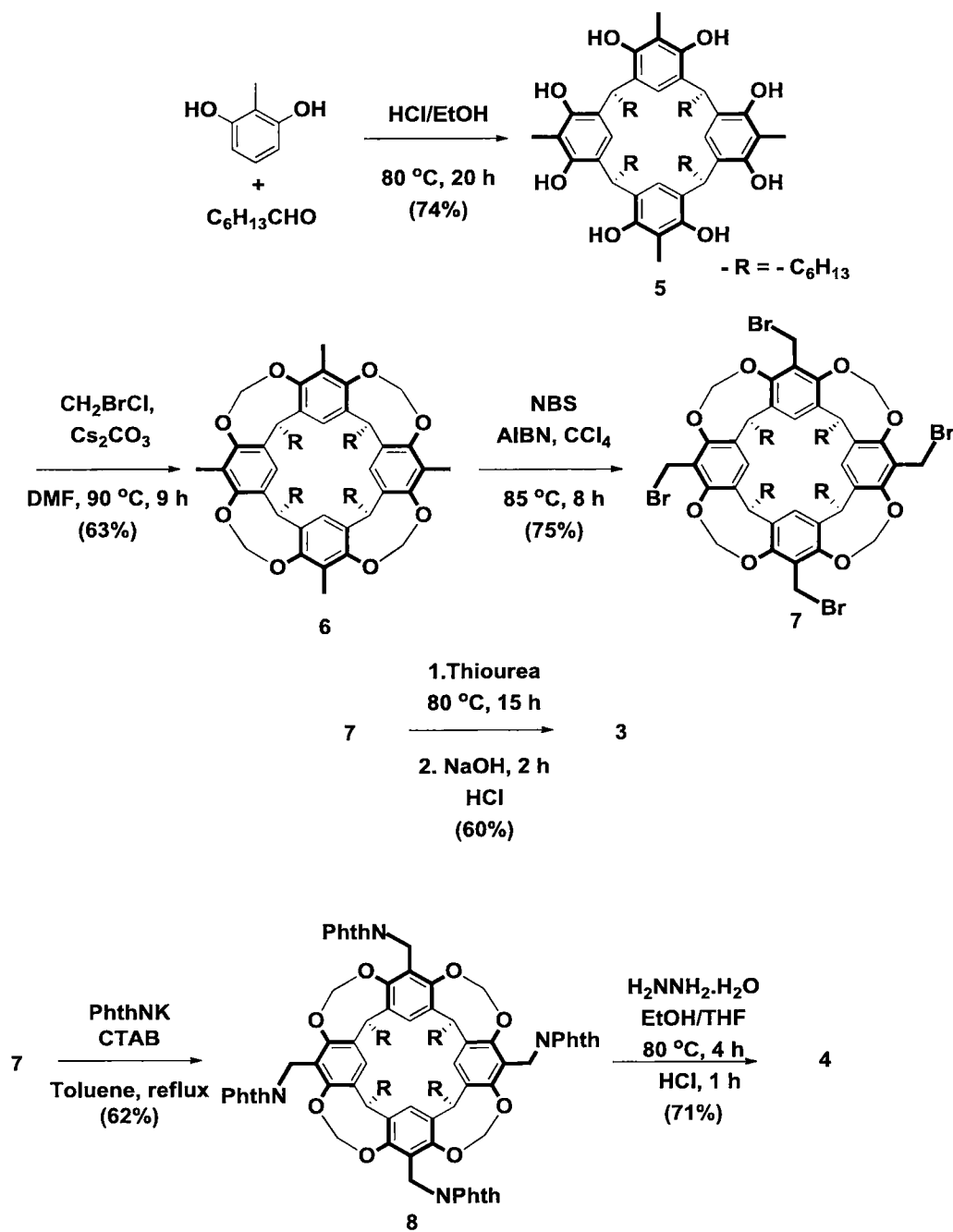


**Figure 5.** Synthesis of resorcinarene thiol and amine surfactants.

## Initial Work

Initially, we synthesized citrate stabilized spherical,<sup>99</sup> and polyvinylpyrrolidone stabilized tetrahedral,<sup>14</sup> platinum nanoparticles (Figure 6) as model nanoparticles. Our investigations showed that citrate stabilized spherical nanoparticles could be phase-transferred from aqueous to organic phase in the presence of linear thiols. However, the strongly bound polyvinylpyrrolidone stabilized nanoparticles could not be phase-transferred even when the incoming linear surfactant was used in excess or with heating. These studies suggest that the choice of the stabilizing surfactant is crucial for the proposed phase-transfer studies of shape-selected nanoparticles.

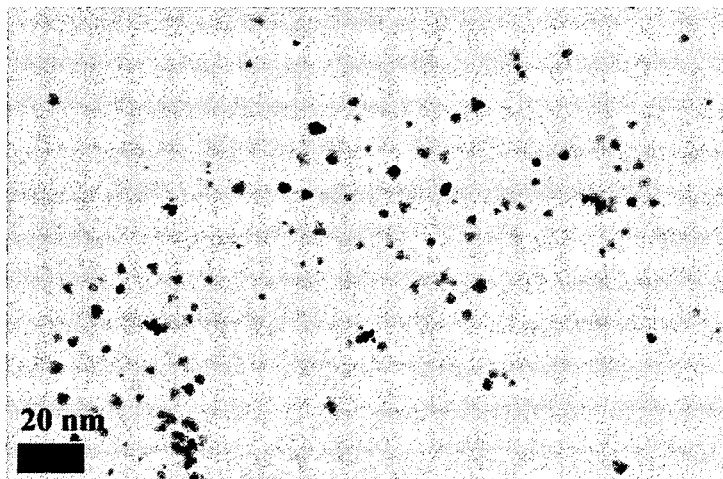


**Figure 6.** TEM image of PVP stabilized tetrahedral platinum nanoparticles.

## **Synthesis and Phase Transfer of CTAB Stabilized Cuboctahedral and Cubic Platinum Nanoparticles**

Platinum nanoparticles of cubic and cuboctahedral shapes<sup>12</sup> (Figure 7) were synthesized by slightly modifying the literature procedures. When compared to strongly interacting polyvinylpyrrolidone, tetraalkylammonium ion interactions are weakly<sup>12</sup> bound on Pt nanoparticle surfaces. Hence we synthesized CTAB stabilized cubic and cuboctahedral<sup>12</sup> platinum nanoparticles by modifying literature procedures. Subsequent to the synthesis, the excess CTAB surfactant was removed by repeated precipitation-dispersion of these nanoparticles under centrifugation conditions. Consistent with the observation of Lee and coworkers<sup>12</sup> our synthesis resulted in a much higher percentage of cuboctahedral nanoparticles than cubic nanoparticles. They showed that while the “cuboctahedral nanoparticles” synthesized consisted of 91% cuboctahedra, the “cubic nanoparticles” synthesized contained only 73% of perfectly cubic nanoparticles.



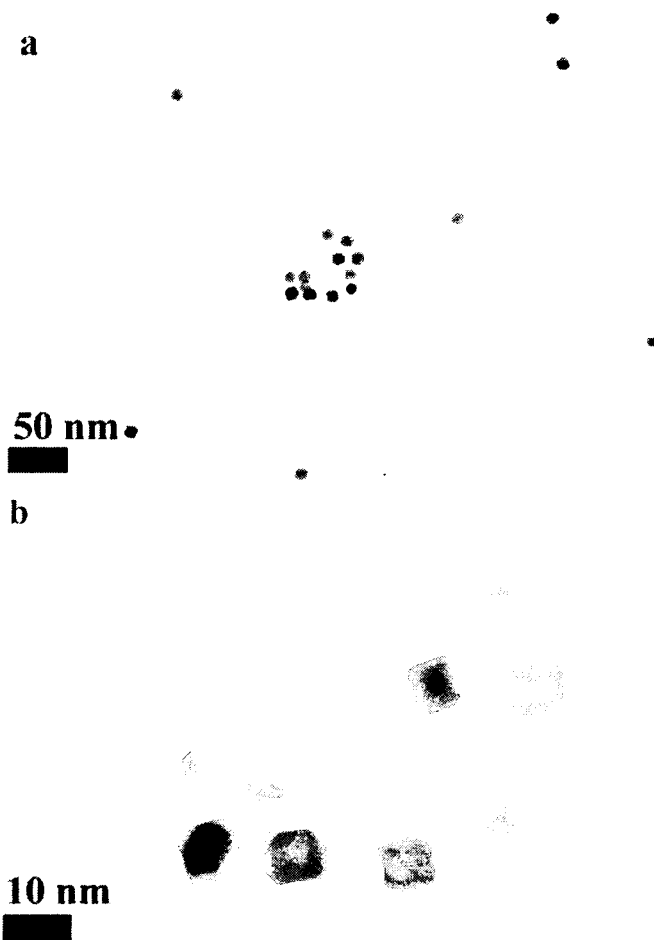


**Figure 7.** Low (a) and High (b) resolution TEM images of CTAB stabilized cuboctahedral platinum nanoparticles.

The procedure developed by Balasubramanian *et. al.*<sup>93</sup> was used to extract CTAB stabilized cuboctahedral/cubic platinum nanoparticles into the organic phase using resorcinarene surfactants as ligands to replace the CTAB. Briefly, CTAB stabilized aqueous dispersions of nanoparticles (2 mL) and tetrahydrofuran solutions (2 mL) of resorcinarene surfactants **3** or **4** (4.5 mM) were mixed vigorously in a silanized dry test tube for a short duration (10 s). An equal volume (2 mL) of co-solvent (toluene) was then

added which led to a complete transfer of cuboctahedral nanoparticles from the aqueous phase to the toluene layer (Figure 8). Phase transfer could be monitored visually by change of colors in the aqueous and organic layers. The color of the organic layer changed from colorless to light brown. An aliquot of the organic solution was drop-casted, dried on a formvar-carbon grid and analyzed by TEM (Figure 9). On the other hand, only resorcinarene thiol **3** was capable of transferring cubic nanoparticles, while resorcinarene amine **4** could not transfer cubic nanoparticles. The exact reasons for this are not clear at this point.



**Figure 8.** Photographs of resorcinarene thiol (left) and resorcinarene amine (right) extracted cuboctahedral platinum nanoparticles. Upper organic phase (light brown in color), lower aqueous phase (colorless) for both resorcinarene thiol and amine extractions.

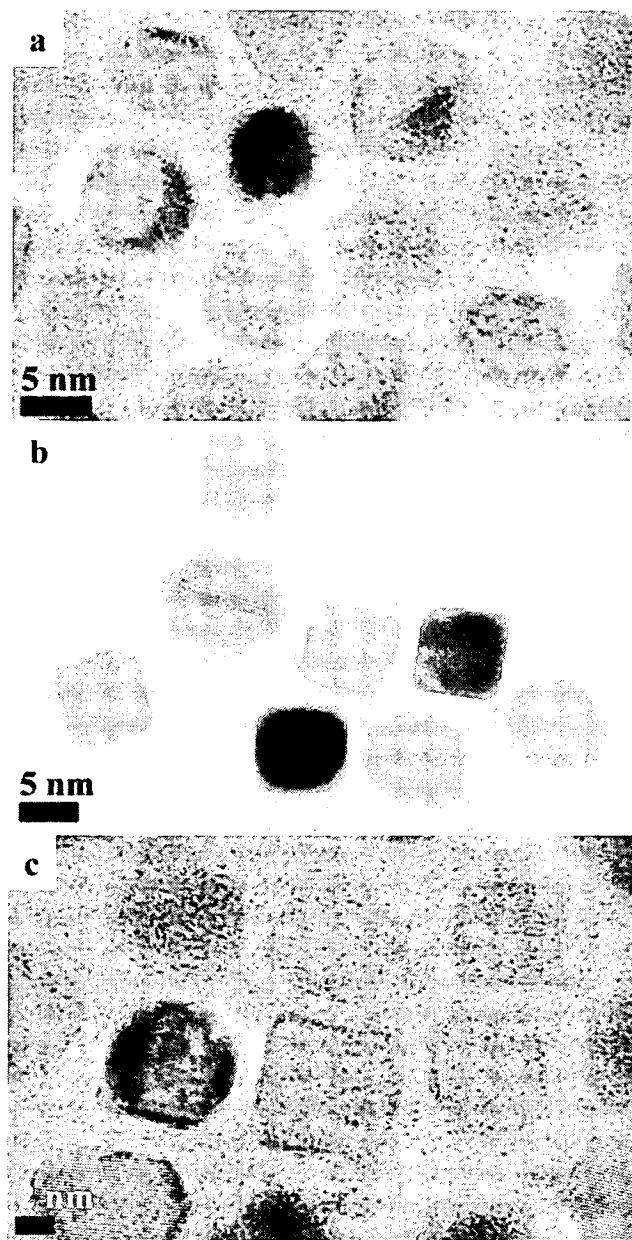


**Figure 9.** TEM images of (a) resorcinarene thiol, (b) resorcinarene amine extracted cuboctahedral platinum nanoparticles and (c) resorcinarene thiol extracted cubic platinum nanoparticles.

Occasionally, with some batches of cuboctahedral nanoparticles the phase-transfer studies were not successful. The nanoparticles were either entirely in the aqueous phase (no phase-transfer at all) or were only partially phase transferred into the organic phase by resorcinarene surfactants. In this case, most of the nanoparticles were in the interface. In such instances, phase-transfer could be completed by using miniscule amounts (0.1 mL) of conc. HCl. Alternately some batches of aqueous cuboctahedral nanoparticle dispersions were mixed with resorcinarene surfactant solutions in THF and refluxed for 20 min under Ar atmosphere to facilitate the ligand exchange process. Subsequent addition of toluene resulted in the extraction of nanoparticles into the organic phase. Though this approach was effective for resorcinarene thiol extraction, it was not successful with resorcinarene amine surfactants. The exact reasons are not clear at this point.

### **Solvent Effect on Phase Transfer**

To probe the importance of solvent in the above extraction, we extracted cuboctahedral nanoparticles using chloroform as co-solvent instead of toluene. In the past, it has been shown that chloroform<sup>93</sup> is a better solvent for the extraction of gold nanoparticles when compared to toluene. Although chloroform could completely extract cuboctahedral platinum nanoparticles into the organic phase, there were significant differences in the composition of the nanoparticle extractions as monitored by <sup>1</sup>H-NMR. In this experiment, the extracted nanoparticle dispersions obtained with various solvents (i.e., in the presence of toluene or chloroform) were evaporated under reduced pressure and redispersed in deuterated chloroform. While the <sup>1</sup>H-NMR spectrum (Figure 10a) of

the cuboctahedral nanoparticles extracted with toluene did not show any noticeable amount of CTAB, the nanoparticle dispersions extracted with chloroform (Figure 10b) showed the presence of CTAB. We believe that this could be due to the solubility of CTAB in chloroform.

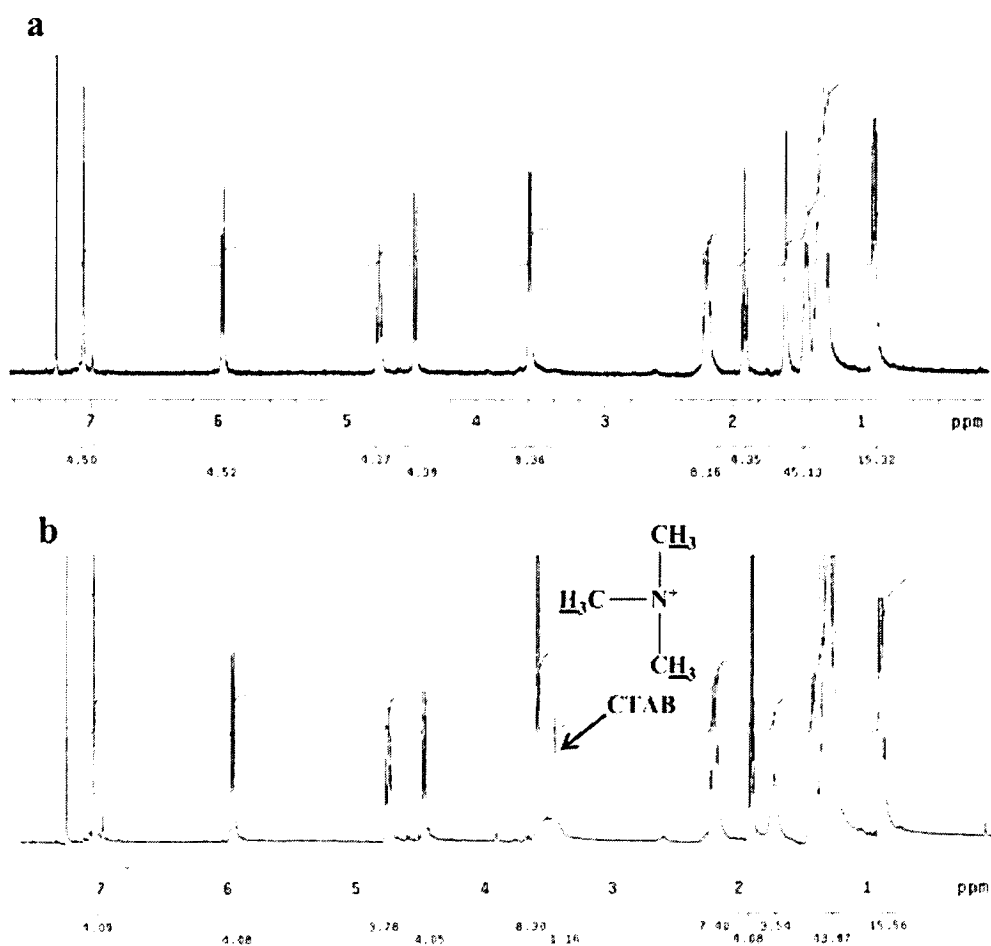


**Figure 10.**  $^1\text{H}$ -NMR spectra of resorcinarene thiol extraction of cuboctahedral platinum nanoparticles carried out in (a) toluene and (b) chloroform.

Though the  $^1\text{H}$ -NMR data confirms the definitive presence of CTAB in the dispersion, its exact location, i.e., whether CTAB is still bound to the nanoparticle surfaces or it is merely present in the solution cannot be unambiguously established. These experiments clearly show that in phase-transfer experiments, there is a need to balance the extraction capability of the solvent with issues such as unintended solubility of initial ligands or incomplete ligand exchange etc. All phase-transfer studies described henceforth are from extraction experiments which used toluene as a co-solvent.

### **Precipitation-Redispersion of Resorcinarene Surfactant Extracted Nanoparticles**

Excess resorcinarene surfactants were used in the above extractions and the resulting nanoparticle dispersions contain excess resorcinarene surfactants. It is known that the stabilizers used for capping the nanoparticles are in dynamic equilibrium with the free ligands<sup>43</sup> present in the solvent. Excess resorcinarene surfactants were removed by selective precipitation of the nanoparticles. Nanoparticle dispersions were evaporated, and the residue obtained was redispersed in small amounts of chloroform (0.5 mL). Nanoparticles could be precipitated from such concentrated dispersions by the addition of a poor solvent such as ethanol (9.5 mL). The complete precipitation of nanoparticles and their separation from excess surfactants was achieved by centrifugation. The precipitate obtained could be completely redispersed in chloroform by gentle shaking.

### Available Surface Area for Catalysis

To evaluate the available surface area on resorcinarene thiol and amine coated cuboctahedral platinum nanoparticles we employed the fluorescence based assay developed by Katz and coworkers.<sup>100</sup> This method uses 2-naphthalenethiol (2NT) as a chemisorptive fluorescent probe for the measurement of the available surface area on the nanoparticles.

Small amounts of 2NT in dichloromethane (0.05 mM) was added to the resorcinarene surfactant (thiol or amine) extracted and precipitated cuboctahedral platinum nanoparticles in dichloromethane. Fluorescence data (Figure 11) showed that until a sufficient concentration of 2NT was reached, the fluorescence was quenched due to its coating on the available surface of the Pt nanoparticles. After a threshold concentration, an increase in the concentration of 2NT led to an increase in the emission intensity due to unbound 2NT. Preliminary experiments indicate that under identical experimental conditions for both resorcinarene thiol and amine extracted nanoparticles i.e., when the same amount of nanoparticles was used for extraction, surfactant concentration, precipitation-redispersion etc., we did not observe any significant difference in the threshold concentration of 2NT after which the fluorescence intensity showed a linear increase with 2NT concentration. Based on these preliminary results, we believe that there are no significant differences in the available surface area of resorcinarene thiol and amine coated platinum nanoparticles.

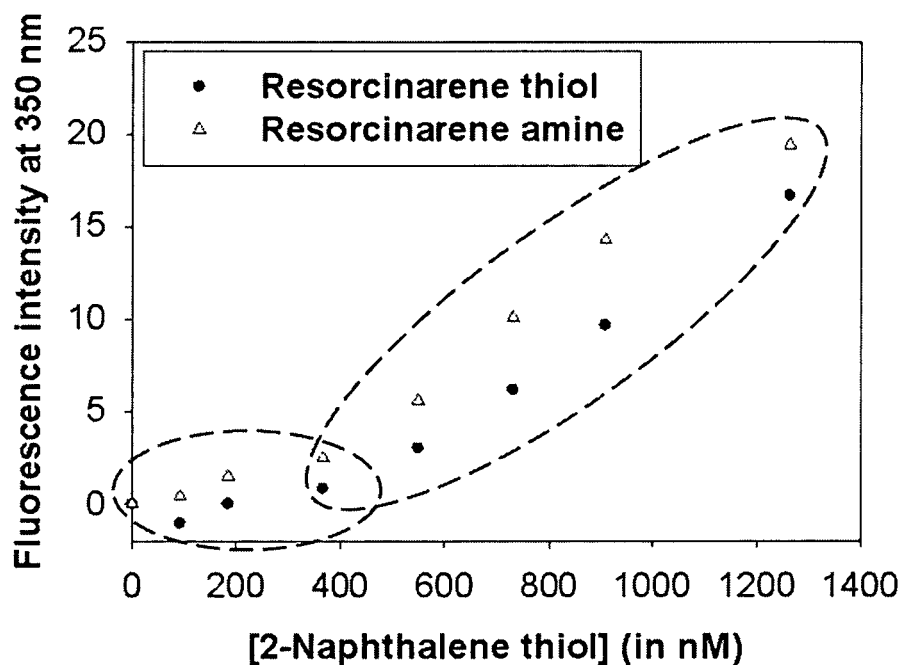


**Figure 11.** Surface area measurement of platinum nanoparticles stabilized with resorcinarene thiol **3** and resorcinarene amine **4**. Small amounts of 2NT were added and fluorescence emission was monitored at 350 nm after excitation at 283 nm. Spectra were normalized at 450 nm.

### **Catalytic Hydrogenation of Allyl alcohol to Propanol using Resorcinarene Surfactant Stabilized Cuboctahedral Nanoparticles**

To study the role of multidentate ligands in catalysis, reduction of allyl alcohol to propanol was conducted on cuboctahedral platinum nanoparticles. Unprecipitated samples (i.e., in the presence of excess surfactants) of resorcinarene thiol/amine stabilized cuboctahedral platinum nanoparticles in  $\text{CDCl}_3$  (2 mL) were placed in a scintillation vial. Amount of the catalyst used was 138 - 150  $\mu\text{g}$  and 253  $\mu\text{g}$  for resorcinarene thiol **3** and resorcinarene amine **4** stabilized platinum nanoparticles respectively. Hydrogen gas was



passed in to the vial for 20 min to activate the catalyst. A volume of 47.4  $\mu\text{L}$  (0.7 mmol) of allyl alcohol was added and reaction was conducted for 8 h at room temperature.  $^1\text{H}$ -NMR spectra showed that with resorcinarene thiol **3** stabilized cuboctahedral platinum nanoparticles there was only, a 4 - 6% conversion of allyl alcohol to propanol. In the case of resorcinarene amine **4** stabilized cuboctahedral Pt nanoparticles, > 99% of allyl alcohol was converted to propanol at room temperature. Increasing the amount of resorcinarene thiol stabilized nanoparticles (1.3 mg of catalyst) increased the conversion of allyl alcohol to propanol to 24% (Figure 12a). Note that in these catalytic reactions presence of excess resorcinarene surfactants traces its origin to the extraction conditions.

Catalysis using resorcinarene surfactant stabilized nanoparticles in the absence of excess surfactants (i.e., precipitated samples) under similar catalysis conditions (as described earlier for unprecipitated samples) gave somewhat different results.  $^1\text{H}$ -NMR spectra showed that even with 96  $\mu\text{g}$  of resorcinarene thiol stabilized platinum catalyst, around 14% conversion to propanol was observed. On the other hand > 99% conversion (Figure 12b) was observed for resorcinarene amine stabilized nanoparticles (102  $\mu\text{g}$  of catalyst). Upon increasing the amount of resorcinarene thiol stabilized catalyst (1.0 mg of catalyst) 58% conversion of 0.7 mmol of allyl alcohol was observed after 8 h. This result is remarkable as Kaifer and coworkers have noted that in the reduction of 1.8 mmol of allyl amine in the presence of 5 mg of platinum catalyst ( $\sim 14.1$  nm) only 10% of the substrate was reduced in 1 h. On the other hand, with higher loading of the catalyst (10 mg), after 6 h  $\sim$  > 95% conversion was observed. In our experiments, the observed 58 % conversion was obtained with just  $\sim$  25% of the catalyst loading employed in Kaifer's studies (5 mg of catalyst which showed 10% conversion).

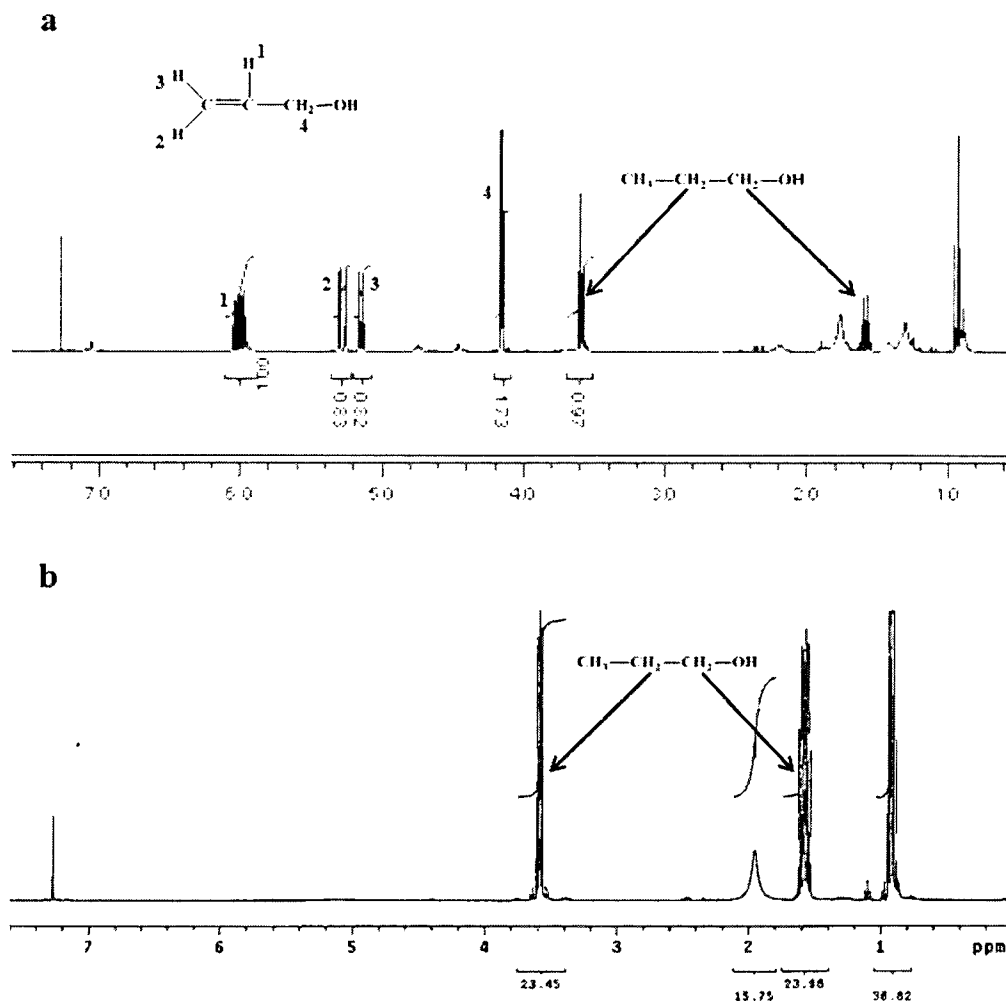


**Figure 12.**  $^1\text{H}$ -NMR spectra of the hydrogenation reactions catalyzed by platinum nanoparticles stabilized with (a) resorcinarene thiol (unprecipitated sample) and (b) resorcinarene amine (precipitated sample).

The stability of the nanoparticles after catalysis experiment was monitored by TEM analysis (Figure 13). In the case of both resorcinarene thiol and resorcinarene amine (Figure 13a) stabilized nanoparticles (unprecipitated samples with excess surfactants), no change in size and shape of the nanoparticles was observed after the catalysis. However, TEM analysis of catalysis reactions carried out with the precipitated samples showed significant ligand dependent differences. While the precipitated resorcinarene thiol (Figure 13b) stabilized nanoparticles were stable after the catalysis, in the case of resorcinarene amine stabilized nanoparticles, substantial aggregation (Figure 13c) was noticed. We believe that this could be due to the weakly binding nature of the amine functional groups.

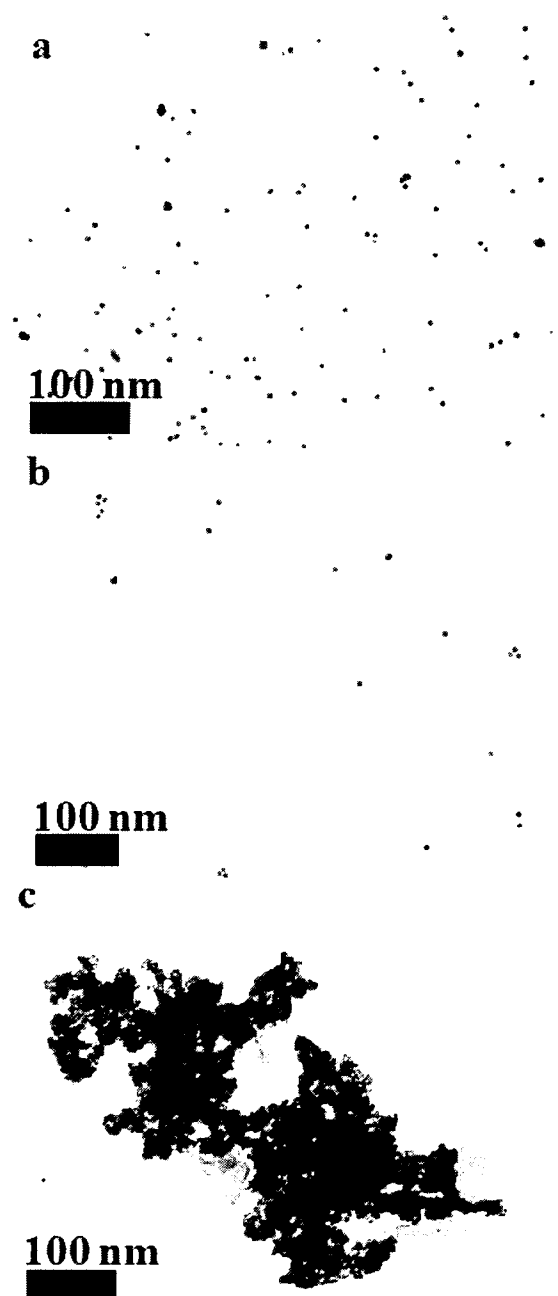


**Figure 13.** TEM analysis of cuboctahedral platinum nanoparticles after catalysis. The stabilizing surfactant and the conditions are (a) resorcinarene amine - unprecipitated sample (b) resorcinarene thiol - precipitated sample and (c) resorcinarene amine - precipitated sample.

Overall, these studies indicate that even in the presence of a miniscule amount of catalyst, resorcinarene surfactant passivated nanoparticles are catalytically active. Remarkably, our study showed that resorcinarene thiol passivated cuboctahedral nanoparticles are catalytically more active when compared to Pt nanoparticles passivated with either linear thiols or other multidentate surfactants such as cyclodextrin. Given the comparable available surface area on both resorcinarene thiol and resorcinarene amine stabilized nanoparticles, the observed differences in catalytic activity between resorcinarene thiol and amine could be due to the bonding/stabilizing of the resorcinarene surfactants to nanoparticles and their stability.

When this work was in progress, Park and coworkers<sup>101</sup> reported the catalytic activity of cubic platinum nanoparticles capped with various strongly and weakly binding ligands. The nanoparticles with various ligands were prepared by ligand-exchange reactions at either room temperature or 50 °C. They investigated the carbon monoxide oxidation reaction using these cubic nanoparticle catalysts and showed that the catalytic activity for the weakly binding tetradecyltrimethylammonium bromide was more than the strongly binding hexadecylthiol or hexadecylamine coated platinum nanoparticles. Catalysis by polyvinylpyrrolidone capped nanoparticles showed intermediate activity.

### **Stabilization and Phase Transfer of Nanodiamonds**

We envisaged the use of resorcinarene surfactants as steric stabilizers for the dispersion stabilization of nanodiamonds in organic solvents. Without any information on the surface composition of the commercially available nanodiamonds or the exact nature of the stabilizers used for their dispersion in aqueous medium, we screened a variety of

resorcinarene molecules such as tetra methyl resorcinarene **5**, tetra methyl cavitand resorcinarene **6**, resorcinarene benzyl thiol **3** and resorcinarene amine **4** as potential steric stabilizers.

We tested the possibility of using the resorcinarene surfactant mediated phase-transfer approach described earlier<sup>93</sup> for the transfer of nanodiamonds into the organic phase. Aqueous nanodiamond dispersion (1 mL) was placed in a clean, dry test tube and mixed with an equal volume of a THF solution of resorcinarene surfactant (6 mM). This solution was sonicated for 20 s, every 15 min over a period of one hour. Subsequently, an equal volume (1 mL) of toluene was added and vortexed for 15 s. Interestingly, we found that only the resorcinarene amine was capable of extracting the nanodiamonds into organic phase immediately after the addition of toluene. The other resorcinarene surfactants failed to extract the nanodiamonds into organic phase.

It is also worth noting that concentration of the resorcinarene amine surfactant played a crucial role in extracting the nanodiamonds from the aqueous to the organic phase. While decreasing the concentration of resorcinarene amine surfactant from 6 mM to 4 mM or 2 mM resulted in the partial extraction of nanodiamonds, with no surfactant (0 mM) there was no extraction of nanodiamonds.

To test the importance of the multidentate macrocyclic skeleton in extracting the nanodiamonds, phase-transfer of nanodiamonds with commercially available (linear and aromatic) amine and ammonium surfactants (Figure 14) was tested. Note that these experiments used a slightly higher concentration of surfactants (48 - 50 mM). Among them only CTAB was partially successful. It could partially extract the nanodiamonds into the organic phase but such dispersions were not stable and the nanodiamonds

eventually went into the interphase. The experiments so far, have unambiguously established the importance of both the amine functionality and the resorcinarene skeleton in the extraction of the nanodiamonds.

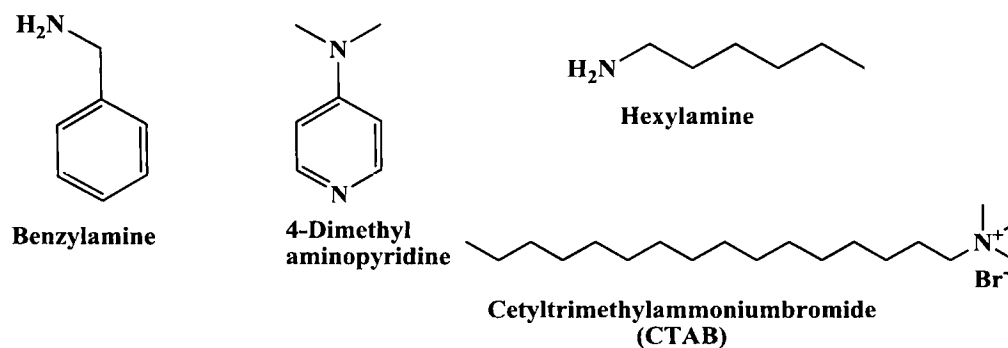


**Figure 14.** Nitrogen containing model surfactants.

Resorcinarene amine **4** coated nanodiamonds could be redispersed in non-polar organic solvents. Nanodiamonds extracted to the organic phase (THF/toluene) were collected into two clean, dry vials (2 mL each) and the volatiles were evaporated in vacuo. The residue obtained in one of the vials was azeotroped (dispersed, concentrated to dryness) with THF and eventually dispersed again in THF. The other sample was similarly dispersed in toluene. Visually such dispersions were stable for at least 4 months (Figure 15).

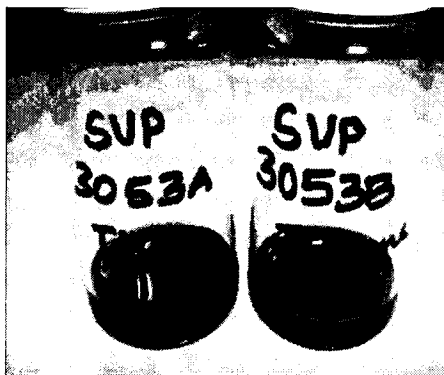


**Figure 15.** Four-month-old dispersions of resorcinarene amine stabilized Microdiamant nanodiamonds in tetrahydrofuran (left) and toluene (right).

#### **Understanding the Extraction of Nanodiamonds by Resorcinarene Amine Surfactant**

FTIR spectroscopy is an important tool in the characterization of functionalized nanodiamonds.<sup>86</sup> To understand the interaction between the surface of nanodiamond and the resorcinarene amine surfactant we used IR spectroscopy. The excess resorcinarene amine used for the extraction of nanodiamonds was removed by a precipitation-redispersion method. Precipitation was achieved by the addition of excess anhydrous ethanol to the concentrated dispersion of nanodiamonds in chloroform. The precipitate was isolated by centrifugation and could be redispersed back in chloroform. Such a redispersed precipitate could be re-precipitated and redispersed in chloroform. Figure 16 shows the FTIR analysis of precipitated and redispersed nanodiamonds, lacking excess resorcinarene amine surfactant.

Careful examination of the FTIR showed that, when compared to resorcinarene amine, the precipitated redispersed nanodiamonds showed

- (i) A new peak at  $1377\text{ cm}^{-1}$ .



- (ii) An increase in the intensity of peak ( $1590\text{ cm}^{-1}$ ).
- (iii) A shoulder at  $1720\text{ cm}^{-1}$ .
- (iv) A broad peak around  $3200\text{ cm}^{-1}$ .

The above data can be explained by assuming the presence of COOH on the nanodiamond surfaces. This is not surprising as during various cleaning procedures, acids are employed which typically leads to the formation of surface COOH acids. The new peak at  $1377\text{ cm}^{-1}$  could be due to the symmetric stretching of  $\text{COO}^-$  group. The increase in the intensity of the peak at  $1590\text{ cm}^{-1}$  was attributed to the antisymmetric stretching of the  $\text{COO}^-$  group. The observation of a shoulder at  $1720\text{ cm}^{-1}$  and a broad peak at  $3200\text{ cm}^{-1}$  could be due to the C=O stretching of the  $\text{COO}^-$  group and the O-H of COOH. This IR data suggests that “as received” Microdiamant nanodiamonds contain surface carboxylic groups and its phase-transfer could have been promoted by the electrostatic stabilization of these carboxylic acid groups by the amine groups of the multidentate aminocavitand surfactants.

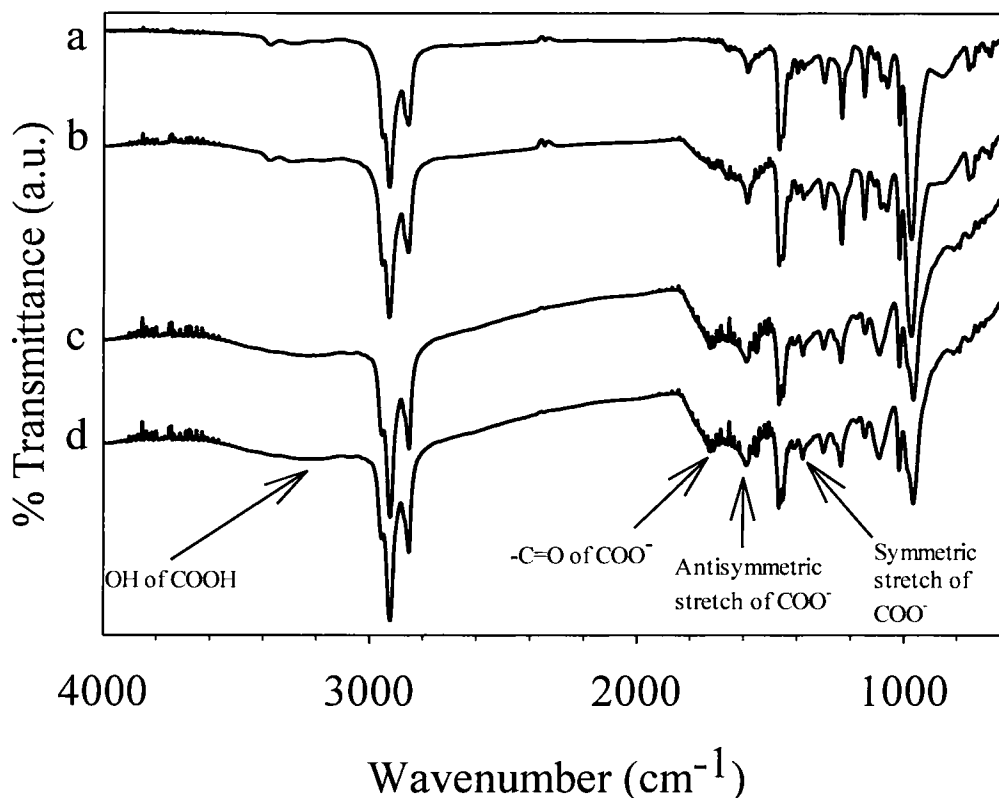


**Figure 16.** FTIR spectra of resorcinarene amine encapsulated and precipitated Microdiamant nanodiamond dispersions. (a) Resorcinarene amine, (b) resorcinarene amine encapsulated Microdiamant nanodiamonds, (c) once and (d) twice precipitated resorcinarene amine encapsulated Microdiamant nanodiamonds.

#### Extraction of Nanodiamonds from Various Commercial Sources

To test the general applicability of the above resorcinarene amine surfactant **4**, phase-transfer experiments were carried out with nanodiamonds from various commercial sources such as Altai, Dynalene and DuPont. The extraction protocol described for the Microdiamant nanodiamond could be readily implemented successfully

for the extraction of nanodiamonds from these sources. Nanodiamonds from various sources showed a clear and complete transfer from the aqueous to the organic phase (Figure 17) except for the DuPont. In the case of DuPont, the nanodiamonds were partially extracted to the organic phase after 2 months.

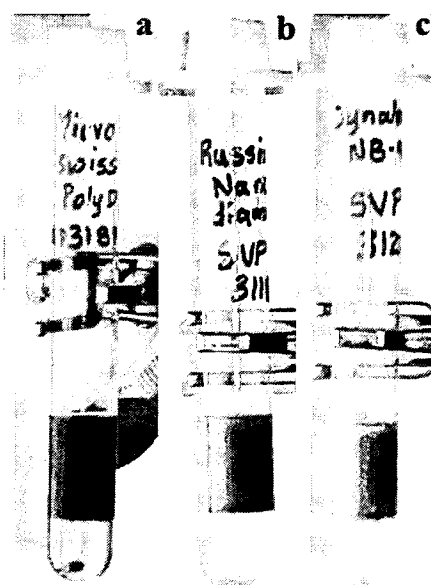


**Figure 17.** Resorcinarene amine extracted (a) Microdiamant, (b) Altai and (c) Dynalene nanodiamonds.

TEM analysis of the nanodiamonds from various sources showed that the nanodiamonds of a variety of sizes and shapes could be extracted in nonpolar organic solvents by the resorcinarene amine surfactant (Figure 18). The nanodiamonds obtained from Altai (a, b) and Dynalene (c, d) were smaller and had an approximate dimension of 4-5 nm, while the Microdiamant nanodiamonds (e, f) were around 30 nm in size. The

DuPont nanodiamonds (g, h) which were extracted slowly were much larger ( $> 100$  nm) and were of irregular shapes.

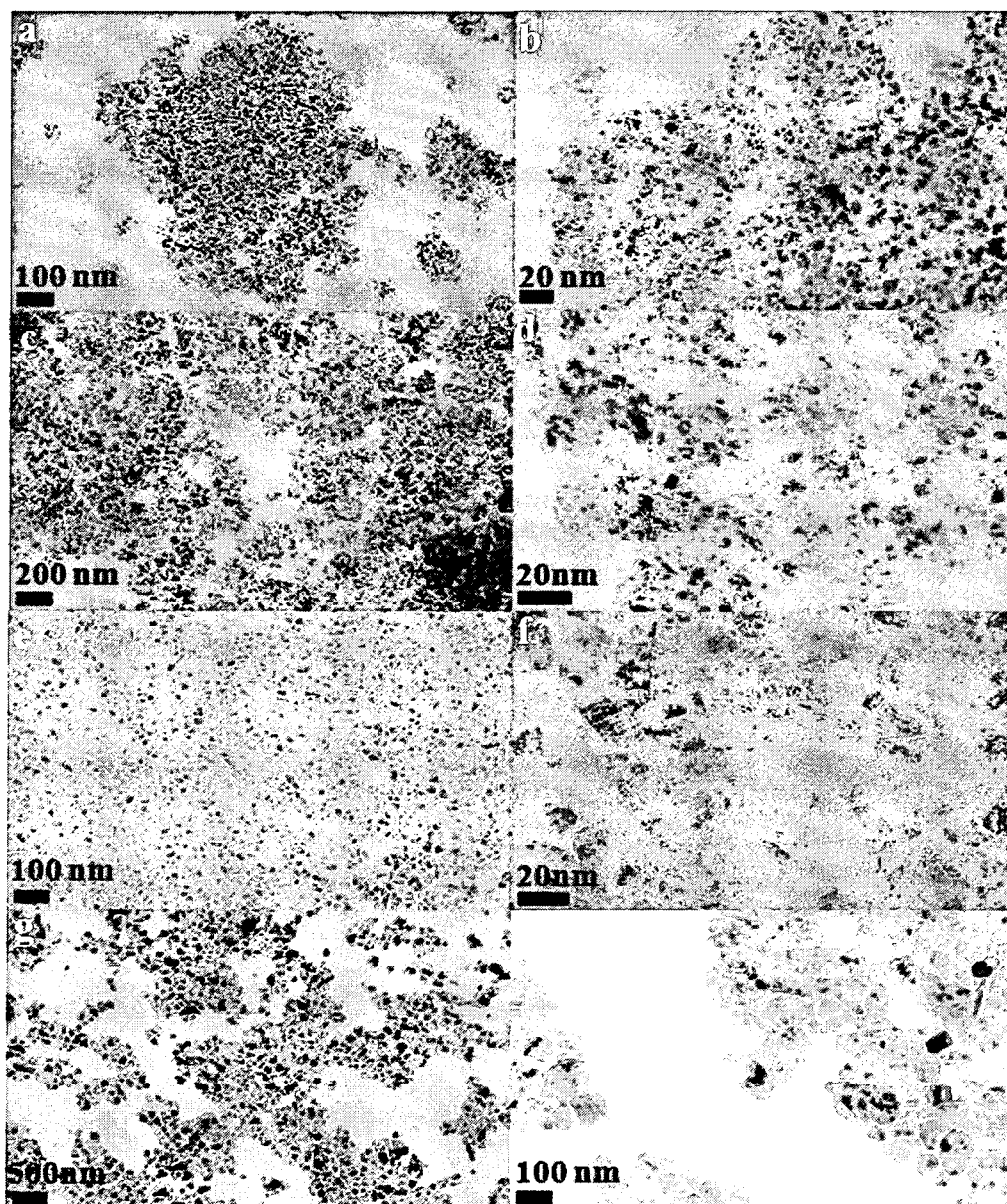


**Figure 18.** TEM analysis of resorcinarene amine extracted (a - b) Altai, (c - d) Dynalene, (e - f) Microdiamant and (g - h) DuPont nanodiamonds.

## **Diamond Film Growth using Resorcinarene Amine Encapsulated Nanodiamonds as Nucleating Agents**

We have shown the utility of these nanodiamonds as nucleating agents in the growth of diamond films in collaboration with Dr. Sacharia Albin's group. Diamond films have found wide ranging applications in electronic and electrochemical devices,<sup>102</sup> sensors,<sup>103</sup> protective coatings,<sup>104</sup> optical windows<sup>105</sup> etc. Despite the recent progress, there are still problems plaguing the development of diamond based electronics, and this requires a reduction in the roughness<sup>106</sup> of diamond films. Nucleation or seeding is required for the fabrication of diamond films on non-diamond substrates. Nanodiamonds have been used as nucleation seeds in chemical vapor deposition (CVD)<sup>107,108,109,110</sup> based growth of diamond films.

Diamond films were grown by the chemical vapor deposition technique on a silicon wafer which was spin-coated with resorcinarene amine encapsulated Microdiamant nanodiamonds as nucleation seeds. In addition to using resorcinarene amine encapsulated nanodiamonds as nucleation seeds, identical films were also grown with a bare silicon surface or by using unmodified (as received) Microdiamant nanodiamond dispersions as seeds. SEM and AFM analysis (Figure 19) showed the formation of continuous diamond films of about 500 nm thickness with both resorcinarene amine modified and unmodified nanodiamond seeds. Remarkably, the grain size of the diamond film in the former was much smaller and more uniform compared to those obtained from as received nanodiamonds. Also, the roughness of the diamond films prepared with resorcinarene amine extracted nanodiamonds as seeds were much less (20.3 nm) when compared to those prepared with as received nanodiamonds as

seeds (roughness = 27 nm). Diamond films without the nanoseeding method only showed sporadic growth of diamond crystals. Such diamond films with reduced roughness are potentially useful in MEMS and several other applications.

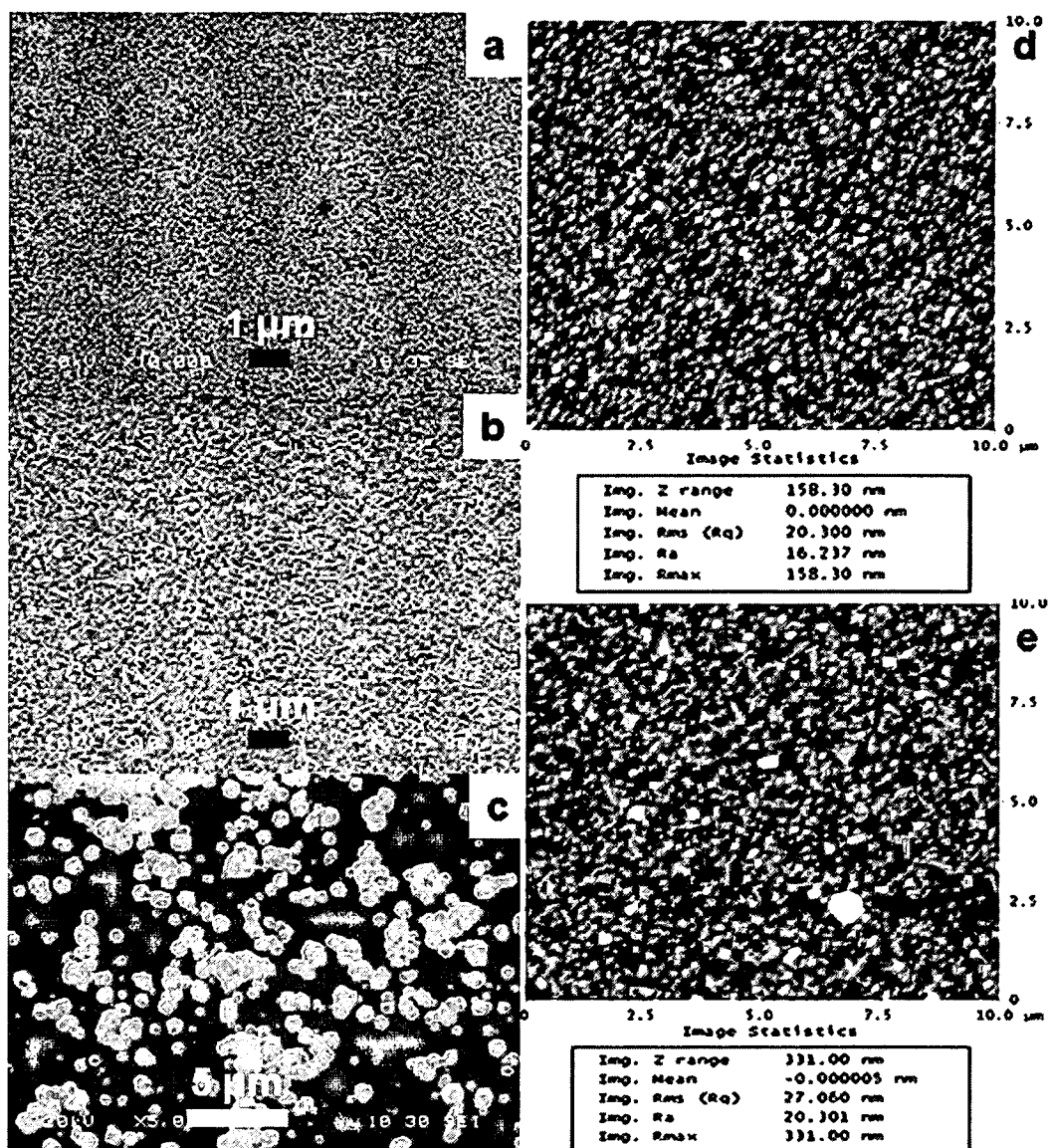


**Figure 19.**<sup>97</sup> SEM (a - c) and AFM (d - e) analysis of diamond films grown with resorcinarene amine encapsulated nanodiamonds (a and d) and unmodified Microdiamant nanodiamonds (b and e) as nucleation seeds and those grown without a nucleating agent (c).

## Experimental Section

Solvents used for this study were dried and distilled using standard procedures. Tetrahydrofuran and toluene were dried and distilled over sodium metal and benzophenone. All the chemicals were purchased from commercial sources and used as such unless specified. Cesium carbonate was dried under vacuum with heating. Moisture sensitive chemicals were handled in a glove box. Organic reactions were conducted under argon atmosphere. TEM analysis of nanodiamond dispersions were done on a JEOL JEM-2100F field emission microscope operating at 200 kV equipped with a Gatan SC1000 ORIUS CCD camera (11megapixel). IR film was made on a salt plate and analyzed on Thermo Electron Nicolet 370 DTGS spectrophotometer. NMR analysis was done on 400 MHz Varian instrument. Sorvall Legend 23R centrifuge was used for centrifugation.

*Synthesis of cuboctahedral and cubic platinum nanoparticles.* Cuboctahedral platinum nanoparticles were synthesized by a slightly modified literature procedure.<sup>12</sup> Briefly, an aqueous solution of potassium tetrachloroplatinate (1.5 mmol) was added to an aqueous solution of CTAB (0.15 mmol) in a round-bottomed flask. The reaction mixture was heated to 50 °C to dissolve the contents. Subsequently it was maintained at room temperature for 5 minutes and ice-cold sodium borohydride (9.6 mmol) solution was added. After 10 minutes, a hydrogen (H<sub>2</sub>) gas balloon was attached to the reaction vessel and the vessel was heated and a temperature of 50 °C was maintained for 6 h. A similar procedure was employed to synthesize the cubic platinum nanoparticles, but the reagents used were K<sub>2</sub>PtCl<sub>4</sub> (1.0 mmol), CTAB (0.1 mmol) and NaBH<sub>4</sub> (31.5 mmol). The product



obtained was centrifuged at 2000 rpm for 15 min to remove larger particles. The supernatant was separated and further centrifuged at 10000 rpm for 30 min. The precipitate obtained was redispersed in water (equal amount as the original dispersion). An aliquot of the precipitated solution was dropcasted, dried on a formvar-carbon grid and analyzed by TEM.

*Synthesis of tetrahedral platinum nanoparticles.*<sup>14</sup> Briefly, 0.25 g of polyvinylpyrrolidone (M.Wt. 360,000) and potassium hexachloroplatinate (2 mL, 0.01 M) were dissolved in 250 mL of nanopure water. The reaction mixture was initially bubbled with argon gas for 20 min. and subsequently with hydrogen gas for 5 min. The resulting solution was sealed with a rubber septum and the flask was wrapped with aluminum foil and kept in the dark. After a day, the reaction mixture became light brown in color. An aliquot of the solution was dropcasted, dried on a formvar-carbon grid and analyzed by TEM.

*Synthesis of spherical platinum nanoparticles.* Briefly, a 10 mM aqueous solution of potassium tetrachloroplatinate (2.5 mL) was aged for 4 days. To this aged solution, sodium citrate (2.9 mg, 9.9 mmol) and nanopure water (47.5 mL) were added. The solution was initially bubbled with argon for 20 min. and subsequently with hydrogen for 5 min. A pale yellow colored solution was obtained after 5 min. The reaction mixture was sealed and kept in the dark for a day. The solution turned black overnight.

*Tetramethyl resorcinarene 5.* 2-methyl resorcinol (30.00 g, 241.66 mmol) was dissolved in ethanol (300 mL) in a three-necked round-bottomed flask. Under argon atmosphere,

heptanal (36 mL, 257.55 mmol) was added to the reaction mixture and the reaction mixture was cooled to 0 °C. Then HCl (30 mL, 12.1 N) was added and the reaction mixture was heated at 80 °C for a day. After cooling to room temperature, the reaction mixture was poured into 500 mL of ice cold water. A yellow precipitate was obtained, which was filtered, and washed with water until the pH of the washings was neutral. The precipitate was dried and dispersed in methanol (approximately three times the weight of the compound) by heating. The solution was cooled to room temperature. The precipitate obtained was filtered to yield tetra methyl resorcinarene as a yellow solid (39.48 g, 74% yield).

<sup>1</sup>H-NMR (DMF-*d*<sub>7</sub>, 400 MHz) δ: 8.96 (s, 8 H), 7.53 (s, 4 H), 4.38 (t, *J* = 7.6 Hz, 4 H), 2.34 (m, 8 H), 2.06 (s, 12 H), 1.34 (m), 0.88 (t, *J* = 6.4 Hz, 12 H).

IR (film, cm<sup>-1</sup>): 3364 (b), 2920, 2850, 1475, 1440, 1335, 1089.

*Tetramethyl resorcinarene cavitand 6.* Tetramethyl resorcinarene (6.03 g, 6.84 mmol) of **5** was dissolved in DMF (200 mL) in a pressure vessel. Bromochloromethane (18 mL, 268.6 mmol), and cesium carbonate (34 g, 104.35 mmol) were added and heated at 90 °C for 11.5 h. After cooling to room temperature, the reaction mixture was poured into a flask containing HCl (340 mL, 2 N) and the crude product was extracted with diethyl ether (4 × 100 mL) and ethyl acetate (100 mL). The organic layer was washed with HCl (2 N, 2 × 130 mL), water (2 × 100 mL), and brine (50 mL), and then dried over magnesium sulfate. The crude product obtained after the removal of the volatiles was purified by silica gel chromatography (ethyl acetate: hexanes 5:95 - 15:85) to yield the title compound as a white solid (3.98 g, 63% yield).

$^1\text{H}$ -NMR ( $\text{CDCl}_3$ , 400 MHz)  $\delta$ : 6.97 (s, 4 H), 5.90 (d,  $J = 6.8$  Hz, 4 H), 4.76 (t,  $J = 8.2$  Hz, 4 H), 4.27 (d,  $J = 7.2$  Hz, 4 H), 2.21 (m, 8 H), 1.97 (s, 12 H), 1.31 (m), 0.89 (t,  $J = 6.8$  Hz, 12 H).

$^{13}\text{C}$ -NMR ( $\text{CDCl}_3$ , 100 MHz)  $\delta$ : 153.42, 138.15, 123.81, 117.77, 98.71, 37.18, 32.09, 30.32, 29.75, 28.14, 22.87, 14.28, 10.54.

IR (film,  $\text{cm}^{-1}$ ): 2927, 2855, 1468, 1429, 1398, 1304, 1233, 1151, 1092, 1021, 978, 756.

*Tetrabromomethylcavitand resorcinarene* **7**. Tetra methyl cavitand resorcinarene **6** (1.6 g, 1.72 mmol) was dissolved in carbon tetrachloride (57 mL) and N-bromosuccinimide (1.83 g, 10.31 mmol) and azo-bisisobutyronitrile (0.289 g, 1.76 mmol) were added and refluxed at 85 °C for 8 h under argon atmosphere. After cooling to room temperature, the reaction mixture was diluted with dichloromethane (150 mL), washed with water (2 100 mL) and dried over magnesium sulfate. The crude product obtained after the removal of the volatiles was purified by silica gel chromatography (ethyl acetate: hexanes 3:97-12:88) which yielded the title compound as white solid (1.61 g, 75% yield).

$^1\text{H}$ -NMR ( $\text{CDCl}_3$ , 400 MHz)  $\delta$ : 7.13 (s, 4 H), 6.04 (d,  $J = 6.4$  Hz, 4H), 4.78 (t,  $J = 8$  Hz, 4 H), 4.57 (d,  $J = 6.8$  Hz, 4H), 4.42 (s, 8 H), 2.21 (m, 8 H), 1.31 (m), 0.90 (t,  $J = 6.8$  Hz, 12 H).

$^{13}\text{C}$ -NMR ( $\text{CDCl}_3$ , 100 MHz)  $\delta$ : 153.42, 137.99, 124.40, 120.86, 99.02, 36.71, 31.71, 29.97, 29.33, 27.70, 22.87, 22.51, 13.93.

IR (film,  $\text{cm}^{-1}$ ): 2928, 2856, 1589, 1471, 1453, 1241, 1148, 1014, 975, 938.

*Resorcinarene benzyl thiol 3*. tetrabromomethyl cavitand resorcinarene **7** (1.46 g, 1.17 mmol) was dissolved in DMF and degassed for 2 minutes, after which thiourea (0.638 g, 8.38 mmol) was added and the mixture was heated at 80 °C for 12 h under argon atmosphere. After cooling the reaction mixture to room temperature a degassed NaOH solution (1 M, 94 mL) was added and the solution was stirred at room temperature for 1.5 h. Then, it was cooled to 0 °C and acidified with HCl to pH 2. The reaction mixture was extracted with EtOAc (3 × 150 mL), and the combined organic layer was washed with water (2 × 100 mL) and dried over magnesium sulfate. The crude product obtained after the removal of the volatiles was purified by silica gel chromatography (ethyl acetate: hexanes 5:95 - 10:90) to yield the title compound as a white solid (0.695 g, 59% yield). Note that in this column, 0.1 mL of AcOH was added to every 100 mL of the elution solvent.

<sup>1</sup>H-NMR (CDCl<sub>3</sub>, 400 MHz) δ: 7.06 (s, 4 H), 5.97 (d, *J* = 6.8 Hz, 4 H), 4.75 (t, *J* = 6.4 Hz, 4 H), 4.48 (d, *J* = 6.8 Hz, 4 H), 3.59 (d, *J* = 7.6 Hz, 8 H), 2.2 (m, 8 H), 1.90 (t, *J* = 7.6 Hz, 4 H), 1.31 (m), 0.90 (t, *J* = 6.8 Hz, 12 H).

<sup>13</sup>C-NMR (CDCl<sub>3</sub>, 100 MHz): δ 152.99, 138.32, 127.35, 119.46, 100.13, 37.17, 32.05, 30.36, 29.69, 28.06, 22.84, 18.34, 14.26.

IR (film, cm<sup>-1</sup>): 2927, 2555, 1469, 1015, 982.

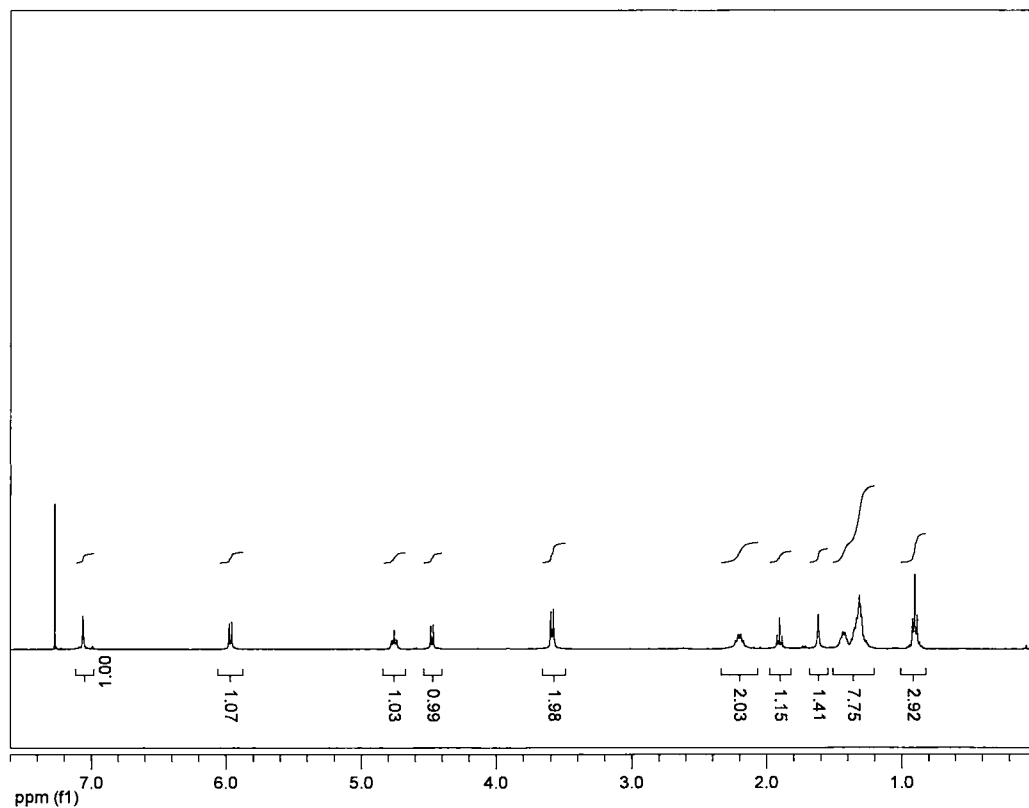


**Figure 20.**  $^1\text{H}$ -NMR of resorcinarene benzyl thiol **3**.

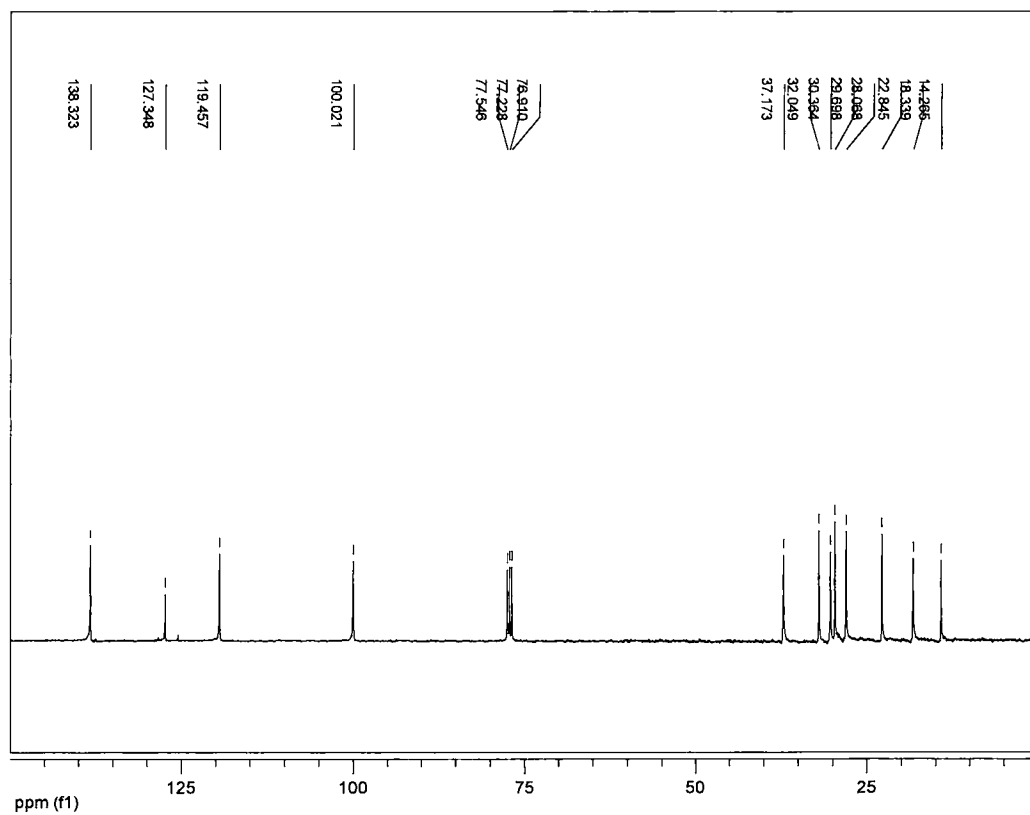


**Figure 21.**  $^{13}\text{C}$ -NMR of resorcinarene benzyl thiol **3**.

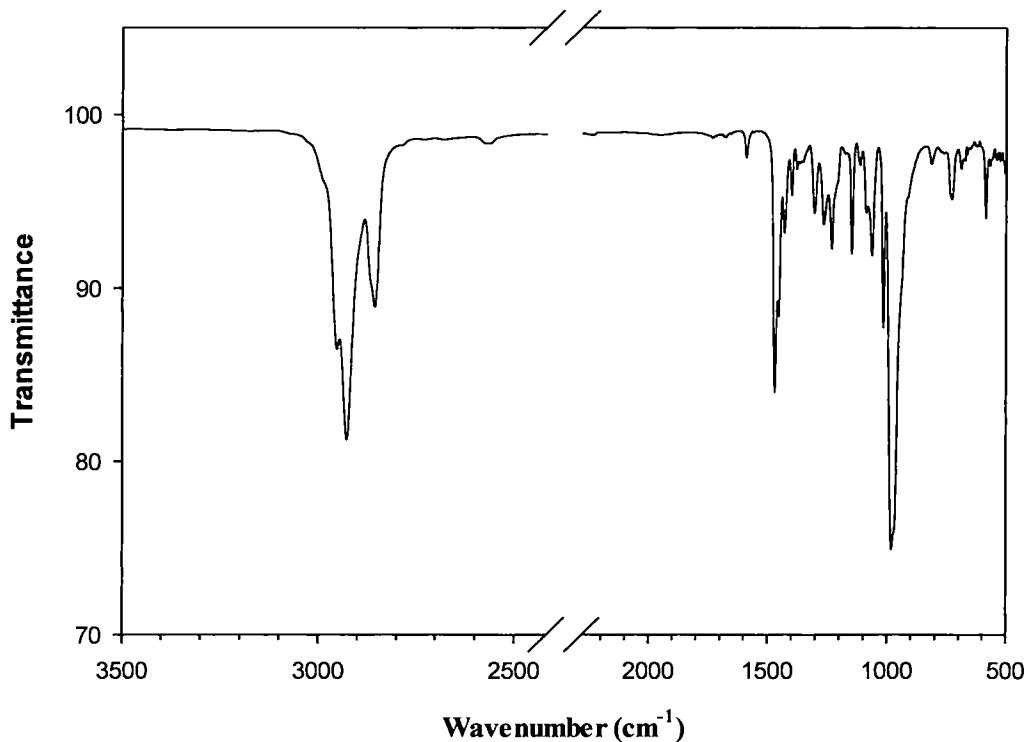


**Figure 22.** FTIR of resorcinarene benzyl thiol **3**.

*Tetraphthalimidomethylcavitand resorcinarene 8.* To tetrabromomethyl cavitand resorcinarene **7** (0.919 g, 0.738 mmol) dissolved in toluene (49.2 mL), potassium phthalimide 0.823 g, (4.44 mmol) and CTAB (0.137 g, 0.375 mmol) were added under argon atmosphere and refluxed for a day. After cooling to room temperature, the reaction mixture was filtered and diluted with chloroform (30 mL). The crude product obtained after evaporation of the volatiles was purified by silica gel chromatography (ethyl acetate: DCM 5:95 - 10:90) to get the title compound as a white colored solid (0.801 g, 72% yield). To eliminate small amounts of aromatic impurity, the compound was re-purified

by another silica gel column (ethyl acetate: hexanes 20:80 - 60:40) to yield the title compound as white solid (0.684 g, 62% yield).

$^1\text{H-NMR}$  ( $\text{CDCl}_3$ , 400 MHz)  $\delta$ : 7.84-7.82 (m, 8 H), 7.73-7.71 (m, 8 H), 7.07 (s, 4 H), 5.79 (d,  $J = 7.2$  Hz, 4 H), 4.68 (t,  $J = 8.4$  Hz, 4 H), 4.66 (s, 8 H), 4.43 (d,  $J = 7.2$  Hz, 4 H), 2.15 (m, 8 H), 1.31 (m), 0.86 (t,  $J = 6.8$  Hz, 12 H).

$^{13}\text{C-NMR}$  ( $\text{CDCl}_3$ , 100 MHz)  $\delta$ : 167.76, 153.68, 137.70, 133.75, 131.87, 123.14, 120.91, 119.92, 99.45, 36.63, 32.57, 31.61, 30.13, 29.34, 27.62, 22.42, 13.83.

IR (film,  $\text{cm}^{-1}$ ): 2928, 2856, 1774, 1717, 1468, 1391, 1234, 1148, 1015, 982.

*Resorcinarene amine 4*. To tetraphthalimidomethyl cavitand resorcinarene **8** (0.960 g, 0.636 mmol) dissolved in a mixture of THF (9.1 mL) and ethyl alcohol (81.7 mL) hydrazine monohydrate (0.620 mL, 12.78 mmol) was added and refluxed under argon atmosphere for 4 h. After cooling to room temperature, the reaction mixture was acidified with HCl (12.1 N, 0.78 mL) and refluxed for an hour. The volatiles were removed under vacuum and a NaOH solution (1.57 g, 2 M) was added. The precipitate obtained was filtered and dried under vacuum to obtain the title compound as a white solid (0.449 g, 71% yield).

$^1\text{H-NMR}$  ( $\text{CDCl}_3$ , 400 MHz)  $\delta$ : 7.04 (s, 4 H), 5.92 (d,  $J = 7.2$  Hz, 4 H), 4.75 (t,  $J = 8$  Hz, 4 H), 4.36 (d,  $J = 6.4$  Hz, 4 H), 3.60 (s, 8 H), 2.20 (q,  $J = 8$  Hz, 8 H), 1.32 (m), 0.90 (t,  $J = 6.8$  Hz, 12 H).

$^{13}\text{C-NMR}$  ( $\text{CDCl}_3$ , 100 MHz)  $\delta$ : 153.23, 138.38, 129.29, 119.27, 99.57, 37.17, 36.33, 32.06, 30.36, 29.71, 28.12, 22.84, 14.26.

IR (film,  $\text{cm}^{-1}$ ): 3374, 2928, 2856, 1587, 1469, 977.



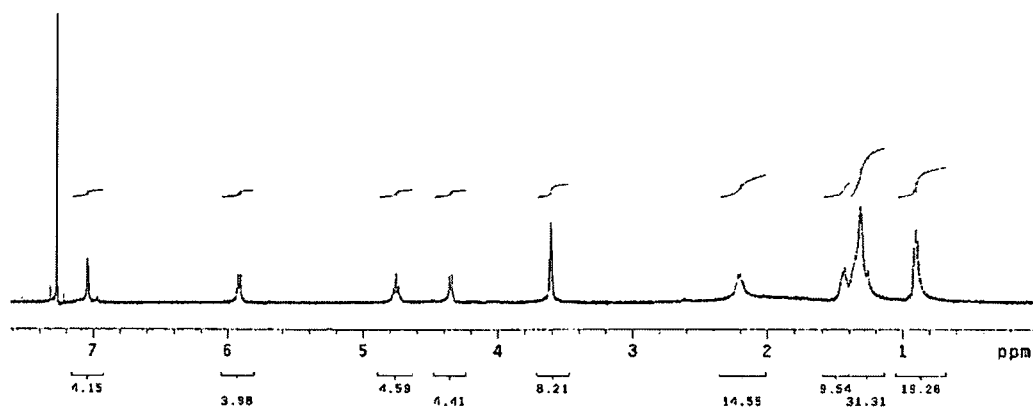


**Figure 23.** <sup>1</sup>H-NMR of resorcinarene amine 4.

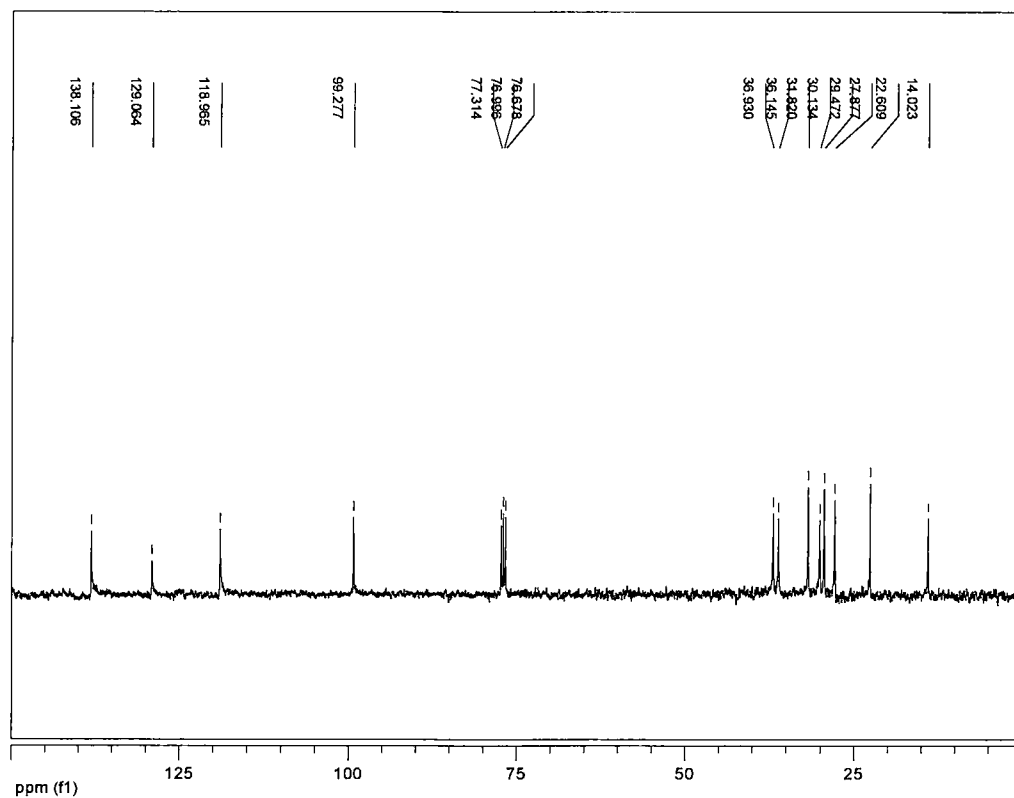


**Figure 24.** <sup>13</sup>C-NMR of resorcinarene amine 4.

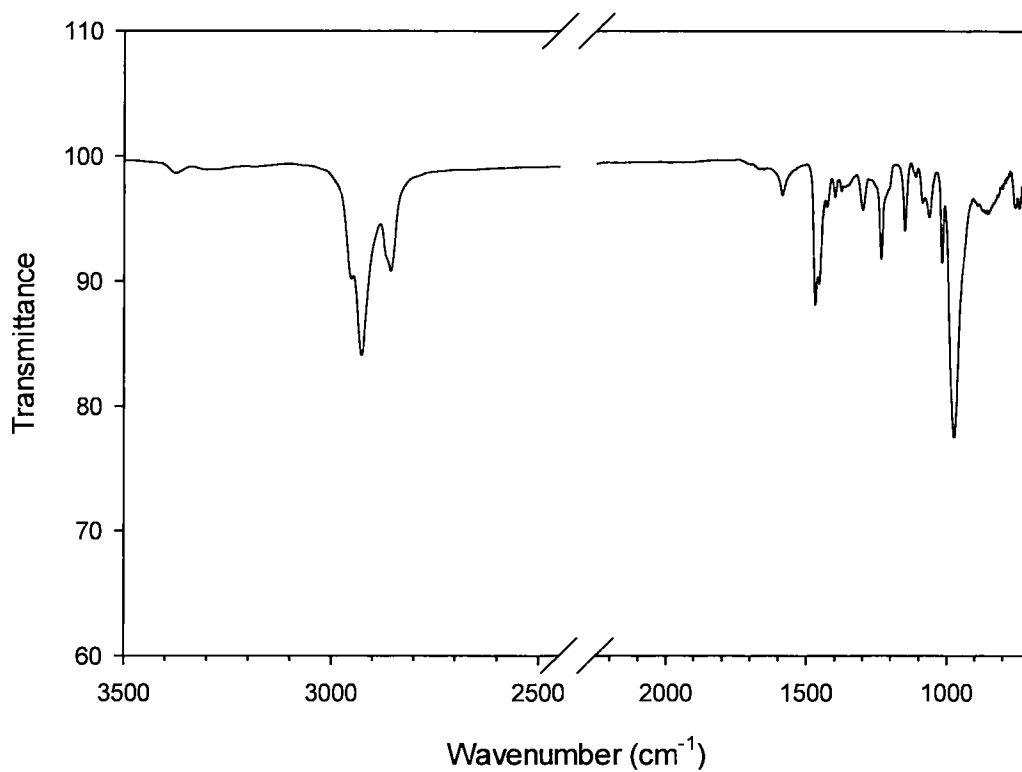


**Figure 25.** FTIR of resorcinarene amine **4**.

## CHAPTER III

### CONCLUSIONS

#### Conclusions for Catalysis Work

In conclusion, we have investigated the influence of multidentate resorcinarene ligands on the catalytic activity of cuboctahedral platinum nanoparticles. Resorcinarene thiol **3** and resorcinarene amine **4** were synthesized by multi-step processes. CTAB stabilized platinum nanoparticles of dominantly cuboctahedral shape were synthesized in the aqueous phase. A phase-transfer method was developed for the extraction of the cuboctahedral Pt NPs from the aqueous to the organic phase using resorcinarene surfactants.

Resorcinarene surfactant stabilized cuboctahedral Pt NPs were used in the catalytic hydrogenation of allyl alcohol to propanol under a variety of conditions. Such studies showed that resorcinarene thiol and resorcinarene amine coated platinum nanoparticles are very active catalysts, and both contain almost comparable surface area for catalysis. However, it was found that thiol extracted cuboctahedral platinum nanoparticles are less active than resorcinarene amine coated nanoparticles. This could be due to the weaker binding of amine groups onto the surface of nanoparticles when compared to the thiol groups. In the absence of excess surfactant, though resorcinarene amine coated nanoparticles led to > 99% of the product, the catalytic nanoparticles aggregated substantially during catalysis. On the contrary, the resorcinarene thiol coated nanoparticles showed a modest 58% conversion, but the catalytic nanoparticles were well dispersed at the end of the catalysis. Such resorcinarene thiol passivated cuboctahedral

nanoparticles are much more catalytically active than cyclodextrin thiol passivated spherical nanoparticles. Our results unambiguously show that the catalytic activity of the nanoparticle can indeed be increased without compromising on their stability.

### **Conclusions for Nanodiamond Work**

In conclusion, we have shown that resorcinarene amine can extract a variety of commercially available nanodiamonds from an aqueous dispersion and stabilize them in non-polar organic solvents. We have proven the importance of the multidentate resorcinarene amine surfactant in mediating the above phase-transfer by a variety of control experiments. Based on FTIR analysis, we believe that this extraction is aided by the electrostatic stabilization of the nanodiamonds by the resorcinarene amine.

Our collaborators have shown that these resorcinarene amine encapsulated Microdiamant nanodiamonds can act as an excellent nucleation source for the growth of diamond films via the CVD approach. SEM and AFM analysis further proved that the diamond films grown using resorcinarene amine surfactant-coated nanodiamonds have a small grain size and low surface roughness when compared to films obtained from unmodified nanodiamonds.

## REFERENCES

- (1) Kelly, K. L.; Coronado, E.; Zhao, L. L.; Schatz, G. C. *J. Phys. Chem. B* **2003**, *107*, 668.
- (2) Murphy, C. J.; Gole, A. M.; Stone, J. W.; Sisco, P. N.; Alkilany, A. M.; Goldsmith, E. C.; Baxter, S. C. *Acc. Chem. Res.* **2008**, *41*, 1721.
- (3) Shiju, N. R.; Gulians, V. V. *Appl. Catal., A* **2009**, *356*, 1.
- (4) McConnell, W. P.; Novak, J. P.; Brousseau, L. C., III; Fuierer, R. R.; Tenent, R. C.; Feldheim, D. L. *J. Phys. Chem. B* **2000**, *104*, 8925.
- (5) Xia, Y.; Xiong, Y.; Lim, B.; Skrabalak, S. E. *Angew. Chem., Int. Ed.* **2009**, *48*, 60.
- (6) Crooks, R. M.; Zhao, M.; Sun, L.; Chechik, V.; Yeung, L. K. *Acc. Chem. Res.* **2001**, *34*, 181.
- (7) Peng, Z.; Yang, H. *Nano Today* **2009**, *4*, 143.
- (8) Kim, C.; Agasti, S. S.; Zhu, Z.; Isaacs, L.; Rotello, V. M. *Nat. Chem.* **2010**, *2*, 962.
- (9) Narayanan, R. *Molecules* **2010**, *15*, 2124.
- (10) Cao, A.; Lu, R.; Vesper, G. *Phys. Chem. Chem. Phys.* **2010**, *12*, 13499.
- (11) Cheng, W.; Wang, E. *J. Phys. Chem. B* **2004**, *108*, 24.
- (12) Lee, H.; Habas, S. E.; Kwestin, S.; Butcher, D.; Somorjai, G. A.; Yang, P. *Angew. Chem., Int. Ed.* **2006**, *45*, 7824.
- (13) Wang, X.; Xu, S.; Zhou, J.; Xu, W. *J. Colloid Interface Sci.* **2010**, *348*, 24.
- (14) Narayanan, R.; El-Sayed, M. A. *J. Phys. Chem. B* **2004**, *108*, 5726.
- (15) Inaba, M.; Ando, M.; Hatanaka, A.; Nomoto, A.; Matsuzawa, K.; Tasaka, A.; Kinumoto, T.; Iriyama, Y.; Ogumi, Z. *Electrochim. Acta* **2006**, *52*, 1632.
- (16) Ott, L. S.; Finke, R. G. *Coord. Chem. Rev.* **2007**, *251*, 1075.
- (17) Chen, S.; Kimura, K. *J. Phys. Chem. B* **2001**, *105*, 5397.
- (18) Yang, J.; Lee, J. Y.; Too, H.-P. *Anal. Chim. Acta* **2007**, *588*, 34.
- (19) Roucoux, A.; Schulz, J.; Patin, H. *Chem. Rev.* **2002**, *102*, 3757.
- (20) Rao, C. N. R.; Vivekchand, S. R. C.; Biswas, K.; Govindaraj, A. *Dalton Trans.* **2007**, 3728.
- (21) Wang, Y.; Xia, Y. *Nano Lett.* **2004**, *4*, 2047.
- (22) Petroski, J. M.; Green, T. C.; El-Sayed, M. A. *J. Phys. Chem. A* **2001**, *105*, 5542.
- (23) Brust, M.; Walker, M.; Bethell, D.; Schiffrin, D. J.; Whyman, R. *J. Chem. Soc., Chem. Commun.* **1994**, 801.
- (24) Li, Y.; El-Sayed, M. A. *J. Phys. Chem. B* **2001**, *105*, 8938.
- (25) Sarkar, A.; Kapoor, S.; Mukherjee, T. *Res. Chem. Intermed.* **2010**, *36*, 403.
- (26) Turkevich, J.; Stevenson, P. C.; Hillier, J. *Discuss. Faraday Soc.* **1951**, *11*, 55.
- (27) Sastry, M. *Curr. Sci.* **2003**, *85*, 1735.
- (28) Yang, J.; Lee, J. Y.; Ying, J. Y. *Chem. Soc. Rev.* **2011**, *40*, 1672.
- (29) Sarathy, K. V.; Raina, G.; Yadav, R. T.; Kulkarni, G. U.; Rao, C. N. R. *J. Phys. Chem. B* **1997**, *101*, 9876.
- (30) Lala, N.; Lalbegi, S. P.; Adyanthaya, S. D.; Sastry, M. *Langmuir* **2001**, *17*, 3766.
- (31) Garcia-Martinez, J. C.; Crooks, R. M. *J. Am. Chem. Soc.* **2004**, *126*, 16170.
- (32) Karg, M.; Schelero, N.; Oppel, C.; Gradzielski, M.; Hellweg, T.; von, K. R. *Chem. Eur. J.* **2011**, *17*, 4648.
- (33) Ji, M.; Yang, W.; Ren, Q.; Lu, D. *Nanotechnology* **2009**, *20*, 075101/1.

- (34) Gittins, D. I.; Caruso, F. *Angew. Chem., Int. Ed.* **2001**, *40*, 3001.
- (35) McMahon, J. M.; Emory, S. R. *Langmuir* **2007**, *23*, 1414.
- (36) Yang, J.; Lee, J. Y.; Too, H.-P.; Valiyaveetil, S. J. *Phys. Chem. B* **2006**, *110*, 125.
- (37) Gonzales, M.; Krishnan, K. M. *J. Magn. Magn. Mater.* **2007**, *311*, 59.
- (38) Hegde, S.; Chadha, R.; Joshi, S.; Mukherjee, T.; Kapoor, S. *Mater. Chem. Phys.* **2009**, *118*, 118.
- (39) Park, D. K.; Lee, S. J.; Lee, J.-H.; Choi, M. Y.; Han, S. W. *Chem. Phys. Lett.* **2010**, *484*, 254.
- (40) Lee, K.-Y.; Lee, Y.-W.; Lee, J.-H.; Han, S.-W. *Colloids Surf., A* **2010**, *372*, 146.
- (41) An, K.; Alayoglu, S.; Ewers, T.; Somorjai, G. A. *J. Colloid Interface Sci.* **2012**, *373*, 1.
- (42) Fihri, A.; Bouhrara, M.; Nekoueishahraki, B.; Basset, J.-M.; Polshettiwar, V. *Chem. Soc. Rev.* **2011**, *40*, 5181.
- (43) Stowell, C. A.; Korgel, B. A. *Nano Lett.* **2005**, *5*, 1203.
- (44) Eklund, S. E.; Cliffl, D. E. *Langmuir* **2004**, *20*, 6012.
- (45) Tian, N.; Zhou, Z.-Y.; Sun, S.-G. *J. Phys. Chem. C* **2008**, *112*, 19801.
- (46) Tian, N.; Zhou, Z.-Y.; Sun, S.-G.; Ding, Y.; Wang, Z. L. *Science* **2007**, *316*, 732.
- (47) Narayanan, R.; El-Sayed, M. A. *Langmuir* **2005**, *21*, 2027.
- (48) Bratlie, K. M.; Lee, H.; Komvopoulos, K.; Yang, P.; Somorjai, G. A. *Nano Lett.* **2007**, *7*, 3097.
- (49) Vannice, M. A. *Kinetics of Catalytic Reactions*; Springer: New York, 2005.
- (50) Ma, R.; Semagina, N. *J. Phys. Chem. C* **2010**, *114*, 15417.
- (51) Renzas, J. R.; Zhang, Y.; Huang, W.; Somorjai, G. A. *Catal. Lett.* **2009**, *132*, 317.
- (52) May, P. W. *Philos. Trans. R. Soc. London, Ser. A* **2000**, *358*, 473.
- (53) Schrand, A. M.; Hens, S. A. C.; Shenderova, O. A. *Crit. Rev. Solid State Mater. Sci.* **2009**, *34*, 18.
- (54) Kuang-Kai, L.; Chia-Liang, C.; Chia-Ching, C.; Jui, I. C. *Nanotechnology* **2007**, *18*, 325102.
- (55) Yu, S.-J.; Kang, M.-W.; Chang, H.-C.; Chen, K.-M.; Yu, Y.-C. *J. Am. Chem. Soc.* **2005**, *127*, 17604.
- (56) Yu. Dolmatov, V. *Russ. Chem. Rev.* **2001**, *70*, 607.
- (57) Gogotsi, Y.; Welz, S.; Ersoy, D. A.; McNallan, M. J. *Nature* **2001**, *411*, 283.
- (58) Danilenko, V. V. *Superhard Mater.*, **2006**, *9*.
- (59) DeCarli, P. S.; Jamieson, J. C. *Science* **1961**, *133*, 1821.
- (60) Schwertfeger, H.; Fokin, A. A.; Schreiner, P. R. *Angew. Chem., Int. Ed.* **2008**, *47*, 1022.
- (61) Huang, H.; Pierstorff, E.; Osawa, E.; Ho, D. *Nano Lett.* **2007**, *7*, 3305.
- (62) Chen, M.; Pierstorff, E. D.; Lam, R.; Li, S.-Y.; Huang, H.; Osawa, E.; Ho, D. *ACS Nano* **2009**, *3*, 2016.
- (63) Zhang, Q.; Mochalin, V. N.; Neitzel, I.; Knoke, I. Y.; Han, J.; Klug, C. A.; Zhou, J. G.; Lelkes, P. I.; Gogotsi, Y. *Biomaterials* **2011**, *32*, 87.
- (64) Holt, K. B. *Philos. Trans. R. Soc., A* **2007**, *365*, 2845.
- (65) Krueger, A. *J. Mater. Chem.* **2011**, *21*, 12571.
- (66) Zhang, X.-Q.; Chen, M.; Lam, R.; Xu, X.; Osawa, E.; Ho, D. *ACS Nano* **2009**, *3*, 2609.

- (67) Turova, O. V.; Starodubtseva, E. V.; Vinogradov, M. G.; Sokolov, V. I.; Abramova, N. V.; Vul, A. Y.; Alexenskiy, A. E. *Catal. Commun.* **2011**, *12*, 577.
- (68) Osswald, S.; Yushin, G.; Mochalin, V.; Kucheyev, S. O.; Gogotsi, Y. *J. Am. Chem. Soc.* **2006**, *128*, 11635.
- (69) Krueger, A. *Adv. Mater.* **2008**, *20*, 2445.
- (70) Fedyanina, O.; Nesterenko, P. *Russ. J. Phys. Chem. A* **2010**, *84*, 476.
- (71) Kruger, A.; Kataoka, F.; Ozawa, M.; Fujino, T.; Suzuki, Y.; Aleksenskii, A. E.; Vul, A. Y.; Osawa, E. *Carbon* **2005**, *43*, 1722.
- (72) Ozawa, M.; Inaguma, M.; Takahashi, M.; Kataoka, F.; Kruger, A.; Osawa, E. *Adv. Mater.* **2007**, *19*, 1201.
- (73) Pentecost, A.; Gour, S.; Mochalin, V.; Knoke, I.; Gogotsi, Y. *ACS Appl. Mater. Interfaces* **2010**, *2*, 3289.
- (74) Osawa, E. *Diamond Relat. Mater.* **2007**, *16*, 2018.
- (75) Xu, X.; Yu, Z.; Zhu, Y.; Wang, B. *Diamond Relat. Mater.* **2005**, *14*, 206.
- (76) Xu, K.; Xue, Q. *Phys. Solid State* **2004**, *46*, 649.
- (77) Osswald, S.; Yushin, G.; Mochalin, V.; Kucheyev, S. O.; Gogotsi, Y. *J. Am. Chem. Soc.* **2006**, *128*, 11635.
- (78) Mitev, D.; Dimitrova, R.; Spassova, M.; Minchev, C.; Stavrev, S. *Diamond Relat. Mater.* **2007**, *16*, 776.
- (79) Krueger, A.; Lang, D. *Adv. Funct. Mater.* **2012**, *22*, 890.
- (80) Zhang, Q.; Mochalin, V. N.; Neitzel, I.; Knoke, I. Y.; Han, J.; Klug, C. A.; Zhou, J. G.; Lelkes, P. I.; Gogotsi, Y. *Biomaterials* **2010**, *32*, 87.
- (81) Nguyen, T. T.-B.; Chang, H.-C.; Wu, V. W.-K. *Diamond Relat. Mater.* **2007**, *16*, 872.
- (82) Liu, Y.; Gu, Z.; Margrave, J. L.; Khabashesku, V. N. *Chem. Mater.* **2004**, *16*, 3924.
- (83) Mochalin, V. N.; Gogotsi, Y. *J. Am. Chem. Soc.* **2009**, *131*, 4594.
- (84) Chang, I. P.; Hwang, K. C.; Ho, J.-a. A.; Lin, C.-C.; Hwu, R. J. R.; Horng, J.-C. *Langmuir* **2010**, *26*, 3685.
- (85) Li, C.-C.; Huang, C.-L. *Colloids Surf., A* **2010**, *353*, 52.
- (86) Krueger, A.; Boedeker, T. *Diamond Relat. Mater.* **2008**, *17*, 1367.
- (87) Moran, J. R.; Karbach, S.; Cram, D. J. *J. Am. Chem. Soc.* **1982**, *104*, 5826.
- (88) Busi, S.; Saxell, H.; Frohlich, R.; Rissanen, K. *CrystEngComm* **2008**, *10*, 1803.
- (89) Misra, T. K.; Liu, C.-Y. *J. Colloid Interface Sci.* **2007**, *310*, 178.
- (90) Sun, Y.; Yan, C.-G.; Yao, Y.; Han, Y.; Shen, M. *Adv. Funct. Mater.* **2008**, *18*, 3981.
- (91) Balasubramanian, R.; Kalaitzis, Z. M.; Cao, W. *J. Mater. Chem.* **2010**, *20*, 6539.
- (92) Stavens, K. B.; Pusztay, S. V.; Zou, S.; Andres, R. P.; Wei, A. *Langmuir* **1999**, *15*, 8337.
- (93) Balasubramanian, R.; Kim, B.; Tripp, S. L.; Wang, X.; Lieberman, M.; Wei, A. *Langmuir* **2002**, *18*, 3676.
- (94) Han, S.; Sheela, V. P.; Xiao, W.; Balasubramanian, R. *J. Phys. Chem. C (Manuscript under revision)*.
- (95) Wei, A. *Chem. Commun.* **2006**, 1581.
- (96) Alvarez, J.; Liu, J.; Roman, E.; Kaifer, A. E. *Chem. Commun.* **2000**, 1151.

- (97) Sheela, V. P.; Xiao, W.; Han, S.; Zhou, X.; Albin, S.; Balasubramanian, R. *J. Mater. Chem.* **2011**, *21*, 6395.
- (98) Boerrigter, H.; Verboom, W.; Reinhoudt, D. N. *J. Org. Chem.* **1997**, *62*, 7148.
- (99) Wilson, O. M.; Hu, X.; Cahill, D. G.; Braun, P. V. *Phys. Rev. B: Condens. Matter. Phys.* **2002**, *66*, 224301.
- (100) Ha, J.-M.; Solovyov, A.; Katz, A. *Langmuir* **2009**, *25*, 10548.
- (101) Park, J. Y.; Aliaga, C.; Renzas, J. R.; Lee, H.; Somorjai, G. A. *Catal. Lett.* **2009**, *129*, 1.
- (102) Cooper, J. B.; Pang, S.; Albin, S.; Zheng, J.; Johnson, R. M. *Anal. Chem.* **1998**, *70*, 464.
- (103) Albin, S.; Zheng, J.; Cooper, J. B. *Diamond Films Technol.* **1996**, *6*, 241.
- (104) Albin, S.; Watkins, L.; Ravi, K.; Yokota, S. *Appl. Phys. Lett.* **1989**, *54*, 2728.
- (105) Phillips, R.; Wei, J.; Tzeng, Y. *Thin Solid Films* **1992**, *212*, 30.
- (106) Baidakova, M.; Vul, A. *J. Phys. D: Appl. Phys.* **2007**, *40*, 6300.
- (107) Arnault, J. C.; Demuyne, L.; Speisser, C.; Le, N. F. *Eur. Phys. J. B* **1999**, *11*, 327.
- (108) Connell, L. L.; Fleming, J. W.; Chu, H. N.; Vestyck, D. J., Jr.; Jensen, E.; Butler, J. E. *J. Appl. Phys.* **1995**, *78*, 3622.
- (109) Achard, J.; Silva, F.; Tallaire, A.; Bonnin, X.; Lombardi, G.; Hassouni, K.; Gicquel, A. *J. Phys. D: Appl. Phys.* **2007**, *40*, 6175.
- (110) Albin, S.; Zheng, J.; Xiao, B.; Cooper, J. B.; Jeffers, R. B.; Antony, S. *New Diamond Front. Carbon Technol.* **2003**, *13*, 341.



## APPENDIX

Figure 19 was reproduced from “Resorcinarene amine stabilized nanodiamond dispersions in organic solvents: applications in diamond film growth”, *J. Mater. Chem.*, **Sheela, V. P.**; Xiao, W.; Han, S.; Zhou, X.; Albin, S.; Balasubramanian, R.; **2011**, *21*, 6395 by the permission of The Royal Society of Chemistry.

<http://www.rsc.org/AboutUs/Copyright/Permissionrequests.asp>



### Author Use of Own Material in Theses and Dissertations

Authors of articles in RSC journals or chapters in RSC books do not need to formally request permission to reproduce their article or book chapter in their thesis or dissertation. For all cases of reproduction the correct acknowledgement should be given in the caption of the reproduced material. The acknowledgement depends on the RSC publication in which the material was published. The form of the acknowledgement to be included in the caption can be found on the page entitled *Acknowledgements to be used by RSC authors*.

Please ensure that your co-authors are aware that you are including the paper in your thesis.

## VITA

Vara Prasad Sheela  
Department of Chemistry and Biochemistry  
Old Dominion University  
4541 Hampton Blvd.  
Norfolk, VA 23529.

### Education

B.Sc., Biotechnology, Botany & Chemistry, Osmania University, India, May 2005.  
M.Sc., Organic Chemistry, Osmania University, India, May 2007.

### Presentations and Publications

“Multidentate ligand stabilized metallic nanoparticles: Synthesis, mechanistic implications and applications”, American Chemical Society, Balasubramanian, R.; Han, S.; **Sheela, V. P.**; March 25-29, **2012**.

“Aminocavitand encapsulated nanodiamonds: Phase-transfer, dispersion and applications in diamond film growth”, American Chemical Society, **Sheela, V. P.**; Xiao, W.; Han, S.; Zhou, X.; Albin, S.; Balasubramanian, R.; March 27-31, **2011**.

“Resorcinarene amine stabilized nanodiamond dispersions in organic solvents: applications in diamond film growth”, *J. Mater. Chem.*, **Sheela, V. P.**; Xiao, W.; Han, S.; Zhou, X.; Albin, S.; Balasubramanian, R.; **2011**, *21*, 6395.

“Brust-Schiffrin synthesis of V-shaped PdPt nanoparticles using resorcinarene amine surfactant with some mechanistic insights”, *J. Phys. Chem. C*, Han, S.; **Sheela, V. P.**; Xiao, W.; Balasubramanian, R. (*Manuscript under revision*).